29

Wind Turbine Applications

Juan M. Carrasco, Eduardo Galván, and Ramón Portillo
Department of Electronic Engineering, Engineering School, Seville University, Spain

29.1 Wind Energy Conversion Systems

Wind energy has matured to a level of development where it is ready to become a generally accepted utility generation technology. Wind turbine technology has undergone a dramatic transformation during the last 15 years, developing from a fringe science in the 1970s to the wind turbine of the 2000s using the latest in power electronics, aerodynamics, and mechanical drive train designs [1, 2].

Most countries have plans for increasing their share of energy produced by wind power. The increased share of wind power in the electric power system makes it necessary to have grid-friendly interfaces between the wind turbines and the grid in order to maintain power quality.

In addition, power electronics is undergoing a fast evolution, mainly due to two factors. The first one is the development of fast semiconductor switches, which are capable of switching quickly and handling high powers. The second factor is the control area, where the introduction of the computer as a real-time controller has made it possible to adapt advanced and complex control algorithms. These factors together make it possible to have cost-effective and grid-friendly converters connected to the grid [3, 4].

29.1.1 Horizontal-axis Wind Turbine

A horizontal-axis wind turbine is the most extensively used method for wind energy extraction. The power rating varies from a few watts to megawatts on large grid-connected wind turbines.

In relation to the position of the rotor regarding the tower, the rotors are classified as leeward (rotor downstream the tower) or windward (rotor upstream the tower), this last configuration being the most widely used.

These turbines consist of a rotor, a gearbox, and a generator. The group is completed with a nacelle that includes the mechanisms, as well as a tower holding the whole system and hydraulic subsystems, electronic control devices, and electric infrastructure as it is shown in Fig. 29.1 [1]. A photograph of a real horizontal-axis wind turbine is shown in Fig. 29.2. We will briefly explain the above-mentioned devices.

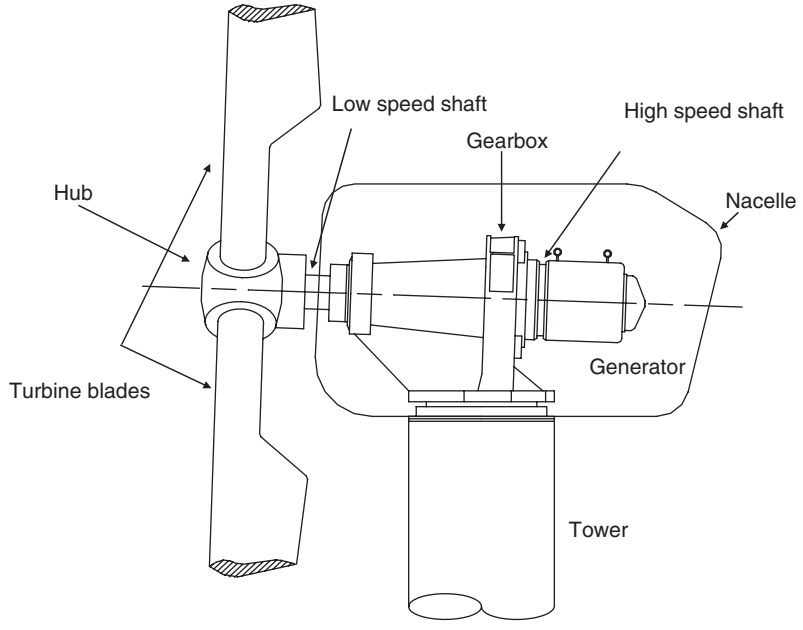

FIGURE 29.1 View of horizontal-axis wind turbine.

FIGURE 29.2 Wind turbine in Monteahumada (Spain). Made S.A. AE-41PV.

29.1.1.1 The Rotor

The rotor is the part of the wind turbine that transforms the energy from the wind into mechanical energy [1]. The area swept by the rotor is the area that captures the energy from the wind. The parameter measuring the influence of the size of the capturing area is the ratio area/rated power. Thus, for the same installed power, more energy will be delivered if this ratio is greater, and so, more equivalent hours (kWh/kW). Values for this ratio close to 2.2 m^2/kW are found today in locations with high average wind speed (>7 m/s), but there is a trend to elevate this ratio above 2.5 m^2/kW for certain locations of medium and low potential. In this case, the technical limits are the high tangential speed at the tip of the blade, that force to lower the speed of the rotors, hence the variable speed and the technology used are most important. Making a bigger rotor for a certain wind turbine involves the possibility of using it for a lower wind speed location by compensating wind loss with a bigger capturing area. The rotor consists of a shaft, blades, and a hub, which holds the fastening system of the blades to the shaft. The rotor and the gearbox form the so-called drive train.

A basic classification of the rotors is between constant pitch and variable-pitch machines, according to whether the type of tie of the blade to the hub is constant or whether it allows rotation to the rotor axis.

The pitch control of a wind turbine makes it possible to regulate energy extraction at high speed wind condition. On the other hand, the use of variable speed makes the systems more expensive to build and maintain.

The use of variable-speed generators (other than 50 Hz of the grid), allows the reduction of sudden load surges.

This condition differentiates between constant speed and variable speed generators. The hub includes the blade pitch controller in case of variable pitch, and the hydraulic brake system in case of constant pitch. The axis to which the hub is tied to the so-called low speed shaft is usually hollow which allows for the hydraulic conduction for regulation of the power by varying the blade pitch or by acting on the aerodynamic brakes in case of constant pitch.

29.1.1.2 The Gearbox

The function of the gearbox, shown in Fig. 29.1, is to adapt a low rotation speed of the rotor axis to a higher one in the electric generator [1, 2]. The gearbox may have parallel or planetary axis. It consists of a system of gears that connect the low speed shaft to the high speed shaft connected to the electric generator by a coupler. In some cases, using multi-pole, the gearbox is not necessary.

29.1.1.3 The Generator

The main objective of the generator is to transform the mechanical energy captured by the rotor of the wind turbine into electrical energy that will be injected into the utility grid.

Asynchronous generators are commonly used in wind turbine applications with fixed speed or variable speed control strategies. Also, in large power wind turbine applications synchronous machines are used. In the asynchronous generator, the electric energy is produced in the stator when the rotating speed of the rotor is higher than the speed of the rotary field of the stator. The asynchronous generator needs to take energy from the grid to create the rotary field of the stator. Because of this, the power factor is decreased and so a capacitor bank is needed. The synchronous generator with an excitation system includes electromagnets in the rotor that generate the rotating field. The rotor electromagnets are fed back with a DC current by rectifying part of the electricity generated. Another kind of generator recently used is the permanent magnet [5]. This type of machine does not need an excitation system, and it is used mainly for low power wind turbine applications. The advantages of using an asynchronous generator are low cost, robustness, simplicity, and easier coupling to the grid, yet its main disadvantage is the necessity of a power factor compensator and a lower efficiency.

29.1.1.3.1 Induction Machine The induction generator, as can be deducted from its torque/speed characteristic, has a nearly constant speed in a wide working torque range, as they are positive (working as a motor) or negative (working as a generator). This characteristic curve is very useful for machines with constant speed, as the machine is autoregulated to keep the synchronous frequency. But the situation is very different when we proceed to change the speed of the generator. It is then necessary to use power converters in order to adapt the generator frequency to the frequency of the grid [3, 6, 7]. The general principles applicable to change the speed of an induction generator can be deduced from the following equation:

$$N_r = N_1 \cdot (1 - s) = \frac{60 \cdot f_1}{p} \cdot (1 - s) \tag{29.1}$$

where N_r is the generator speed (rpm), N_1 is the generator synchronous speed, s is the induction generator slip, p is the pole pair number, and f_1 is the excitation stator frequency (Hz).

From Eq. (29.1), it is immediately inferred that the speed can be controlled in either ways; one way is changing the synchronous speed and the other is changing the slip. The speed is deduced from the number of pole pairs p and the supplying frequency into the machine f_1. The slip can be easily changed when modifying the torque/slip characteristic curve. This modification can be achieved as follows: first, by changing the input voltage of the generator; second, by changing the resistance of the rotor circuit; and third, by injecting a voltage into the rotor so that it has the same frequency as the electromotive force induced in it and an arbitrary magnitude and phase. The techniques used to vary the supplying frequency permit a wide range of variation of the speed, from 0 to 100% or even greater than the synchronous speed. Another variable-speed technique is achieved by changing the number of poles which permit a regulation of the speed in discrete steps. If we proceed to vary the slip, then the range of variation of the speed is within a narrow margin of regulation.

Among all these techniques, only the variation of the voltage can be actually implemented using a squirrel cage machine with a short-circuited rotor. The rest are implemented by means of a wound-rotor machine.

The stator voltage can be varied by means of a power converter [4, 8, 9]. This converter should be connected in series to the generator and to the grid. Since it is only necessary to vary the voltage of the generator and not its frequency, an AC–AC converter can be used. Furthermore, the power converter bears all the power of the generator so it deals with all the disadvantages of the other wide-range of control techniques.

For the speed to be varied by changing the slip, it is necessary to work with wound rotor induction machines.

29.1.1.3.2 Synchronous Machine with Excitation System As it is well-known, the general principle to change the speed of a synchronous machine is summarized in the following equation [3, 6, 7]:

$$N_r = N_1 = \frac{60 \cdot f_1}{p} \tag{29.2}$$

The only way to control the speed is by changing the number of pole pairs or by supplying frequency into the machine, f_1. Therefore, wide range or discrete steps are permitted.

The synchronous machine will always be controlled in a wide range of the rotor speed, ω_r. In this kind of system, the excitation current permits an easier torque and power control.

29.1.1.3.3 Permanent Magnet Synchronous Machine As with the synchronous generator with excitation system, the permanent magnet synchronous machine can be controlled in a wide range of rotor speeds ω_r. In this case, a magnetic field control has to be made from the power converter. The advantage of this machine is better performance and less complexity [3, 6, 7, 10].

29.1.1.4 Power Electronic Conditioner

The power electronic conditioner is a converter that is mainly used in variable speed applications. This converter is connected between the generator machine and the utility grid by an isolating transformer and permits different frequency and voltage levels in its input and output. The power converter is connected to the stator voltage or to the rotor of a wound rotor machine. This system includes large power switches that can be GTOs, Thyristors, IGCTs, or IGBTs arranged in different topologies.

29.1.2 Simplified Model of a Wind Turbine

The mechanical power P_m in the low speed shaft can be expressed as a function of the available power in the wind P_v by the Eq. (29.3):

$$P_m = C_p\,(\lambda, \beta) \cdot P_w \tag{29.3}$$

where $C_p\,(\lambda, \beta)$ is the power coefficient, which is a function of the blade angle β and the dimensionless variable $\lambda = \omega_L R / v_w$ (where ω_L is the angular speed on the low speed shaft, R is the turbine radius, and v_w the wind speed). In Fig. 29.3 an analytical approximation of the power coefficient $C_p(\lambda, \beta)$ is shown.

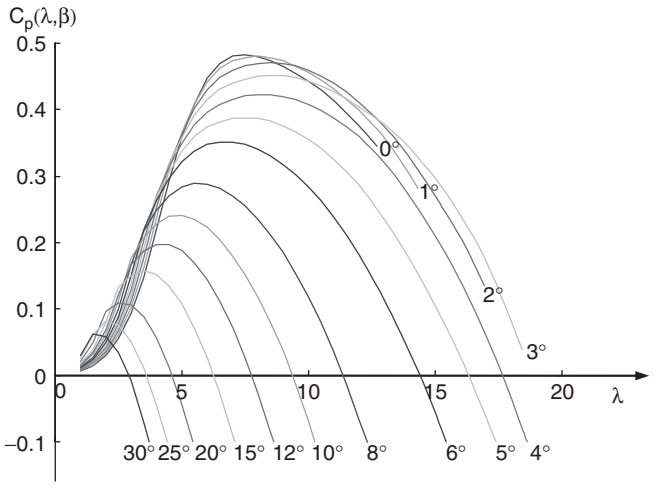

FIGURE 29.3 Analytical approximation of $C_p(\lambda, \beta)$ characteristic (blade pitch angle β as parameter).

In Fig. 29.4 the power characteristic of a wind turbine P_m is shown.

The power of the wind can be expressed by the following equations [1, 2]:

$$P_w = \frac{1}{2}\rho\pi R^2 v_w^3 \tag{29.4}$$

where ρ is the air density.

Substitution of Eq. (29.4) in Eq. (29.3) and including λ in such expression, the following can be obtained:

$$Q_L = \frac{C_p}{2\lambda^3}\rho\pi R^5 \omega_L^2 \tag{29.5}$$

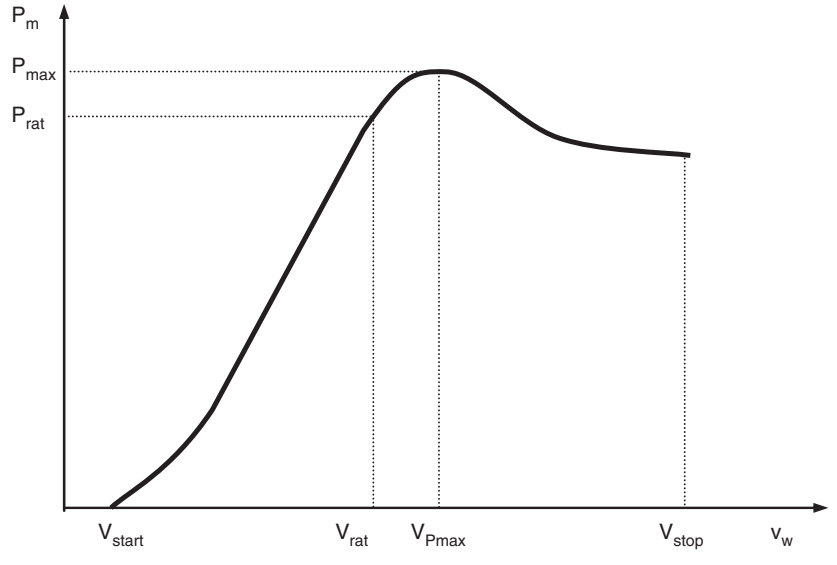

FIGURE 29.4 Power characteristic of the wind turbine.

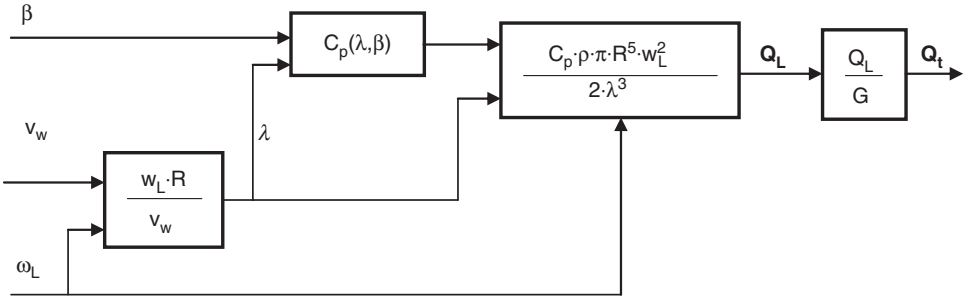

FIGURE 29.5 Torque calculation block diagram.

where Q_L is the torque in the low speed shaft that the wind turbine draws from the wind.

This Eq. (29.5) is represented in Fig. 29.5.

Neglecting mechanical losses, the total torque on the high speed shaft, Q_t is equal to the torque in the low speed shaft, Q_L, divided by the gearbox ratio, G.

$$Q_t = \frac{Q_L}{G} \tag{29.6}$$

Equation (29.7) shows the differential equation for the dynamics of the rotational speed that depends on the difference of load and generator torque.

$$Q_t - Q_e = J\frac{d\omega_r}{dt} \tag{29.7}$$

In Eq. (29.7) J is the total inertia of the system referred to the high speed shaft.

Figure 29.6 shows the block diagram of the simplified mechanical model of a wind turbine. Also, it has been represented by the electrical power P_e, obtained by multiplying the electrical torque Q_e by the rotor speed ω_r and the electrical performance η.

29.1.3 Control of Wind Turbines

Many horizontal axes, grid-connected, and medium- to large-scale wind turbines are regulated by pitch control, and most of the wind turbines built so far have practically constant speed, since they use an AC generator, directly connected to the distribution grid, which determines its speed of rotation.

In the last few years, variable speed control has been added to pitch-angle control design in order to improve the performance of the system [11]. Variable speed operation of a wind turbine has important advantages vs the constant speed ones. The main advantages of variable speed wind tunnel are the reduction of electric power fluctuations by changes in kinetic energy of the rotor, the potential reduction of stress loads on the blades and the mechanical transmissions, and the possibility to tune the turbine to local conditions by adjusting the control parameters. On the other hand, variable speed control is normally used with fixed pitch angle and very few applications using both controls have been reported [12, 13].

In short, four different wind turbine types are provided depending on the controller [14]:

- No control. The generator is directly connected to a constant frequency grid, and the aerodynamics of the blade is used to regulate power in high winds.
- Fixed speed pitch regulated. In this case, the generator is also directly connected to a constant frequency grid, and pitch control is used to regulate power in high winds.
- Variable speed stall regulated. A frequency converter decouples the generator from the grid, allowing the rotor

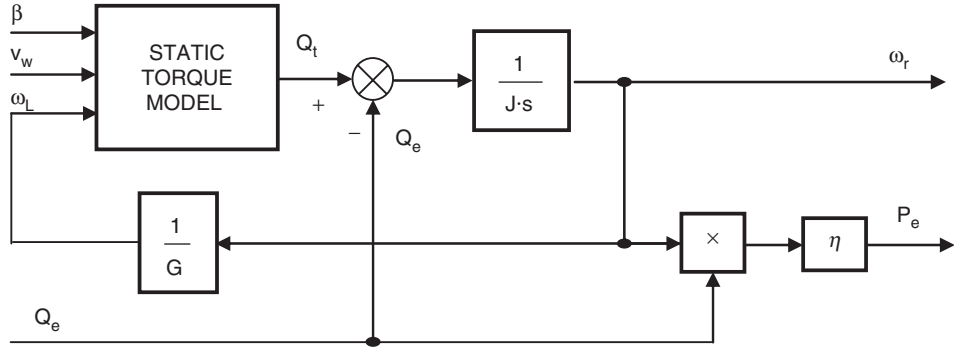

FIGURE 29.6 Mechanical model of a wind turbine.

speed to be varied by controlling the generator reaction torque. In high winds, this speed control capability is used to slow the rotor down until aerodynamic stall limits the power to a desired level [15].

- Variable speed pitch regulated. A frequency converter decouples the generator from the grid, allowing the rotor speed to be varied by controlling the generator reaction torque. In high winds, the torque is held at a rated level, and pitch control is used to regulate the rotor speed, and hence, also the power [13].

A power converter will be mainly used in variable speed applications. In fixed speed control, a power converter could be used for a better system performance, for example, smooth transition during turn on, harmonics, and flicker reduction, etc. Next, the operation of the most general controller, namely, the variable speed pitch regulator controller is explained. Another controller can be obtained from this control scheme, but will not be presented here.

29.1.3.1 Variable Speed Variable Pitch Wind Turbine

Objectives of variable speed control systems are summarized by the following general goals [12, 16, 17]:

- to regulate and smooth the power generated
- to maximize the energy captured
- to alleviate the transient loads throughout the wind turbine
- to achieve unity power factor on the line side with no low frequency harmonics current injection
- to reduce the machine rotor flux at light load reducing core losses

Objectives for the pitch-angle control are similar to the variable speed. If pitch-angle control is used together with variable speed, better performance in the system is obtained. For instance, to permit starting, blade pitch angle differs from the operation pitch angle, allowing an easier starting and optimum running. Moreover, the power and speed can be limited through rotor pitch regulation.

The control diagram is shown schematically in Fig. 29.7. The generator torque Q_e and the pitch angle β control the wind turbine. The control system acquires the actual generated electric power P_e and the generator speed, ω_r, and calculates the reference generator torque Q_e^{ref} and the reference pitch angle β^{ref}, using two control loops [14].

In low winds it is possible to maximize the energy captured by following a constant tip speed ratio λ load line which corresponds to operating at the maximum power coefficient. This load line is a quadratic curve in the torque-speed plane as it is shown in Fig. 29.8. During that time, the pitch angle is adjusted to a constant value, the maximum power pitch angle.

If there is a minimum allowed operating speed, then it is not possible to follow this curve in very low winds, and the turbine is then operated at a constant speed N_{min} shown in Fig. 29.8. On the other hand, in high wind speed, it is necessary to limit the torque Q_{rate} or power P_{rate} of the generator to a constant value.

The control parameters are: the minimum speed ω_r^{min}, the maximum speed in constant tip speed ratio mode ω_r^{max}, the nominal steady-state operating speed ω_r^{rat}, and the parameter K_λ which defines the constant tip speed ratio line $Q_e = K_\lambda \omega_r^2$. K_λ is given by (29.8):

$$K_\lambda = \frac{\pi \rho R^5 C_p(\lambda, \beta)}{2\lambda^3 G^3} \tag{29.8}$$

When the generator torque demand is set to $K_\lambda \omega_r^2$ where ω_r is the measured generator speed, this ensures that in the steady state the turbine will maintain the tip speed ratio λ_{opt} and the corresponding maximum power coefficient $C_p(\lambda, \beta)$.

Figure 29.9 shows the simplified control loops used to generate pitch and torque demands. When operating below rated power, the torque controller is active, and the pitch demand

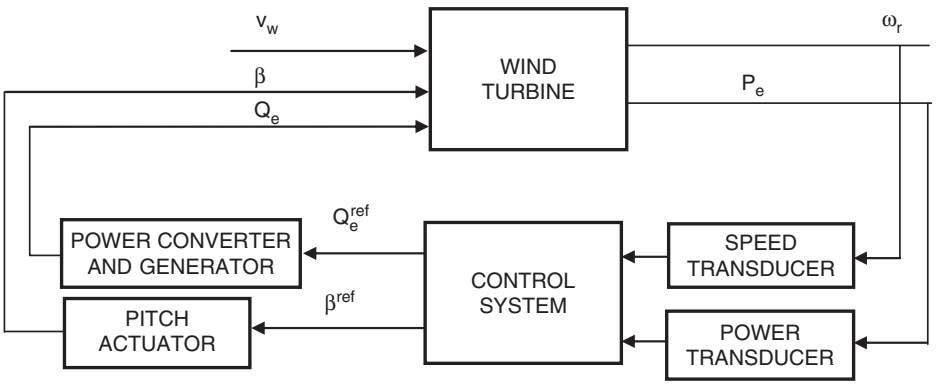

FIGURE 29.7 Block control diagram of the variable speed pitch regulated wind turbine.

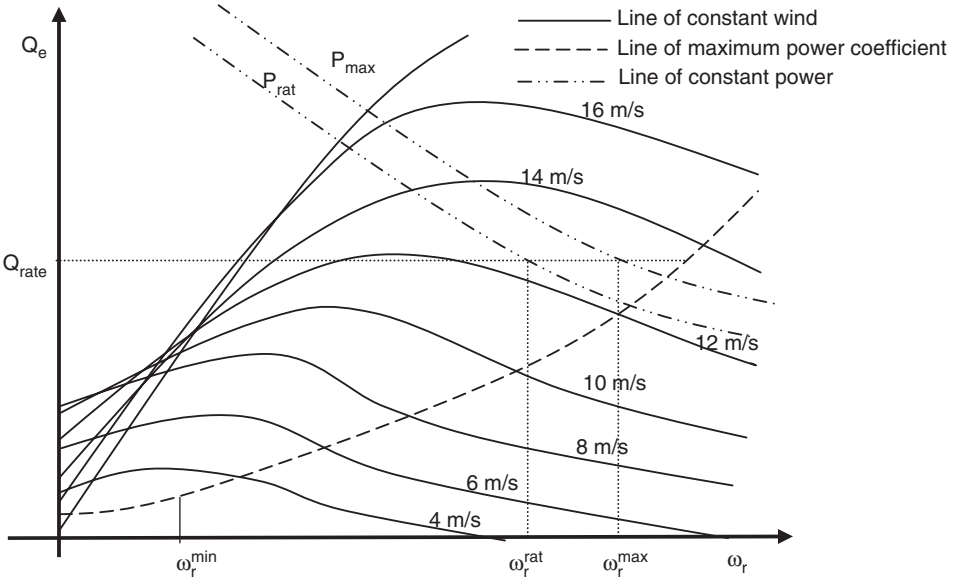

FIGURE 29.8 Variable speed pitch regulated operating curve.

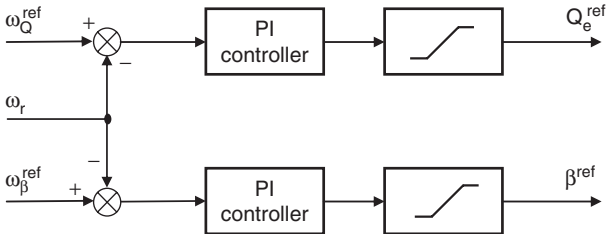

FIGURE 29.9 Pitch regulated variable speed control loops.

loop is active when operating above rated power. Below rated, the speed set-point, ω_Q^{ref}, is the optimum speed given by the optimal tip speed ratio curve and pitch angle is held at zero. Above rated, the reference generator torque is hold rated constant value Q_{rate} and the pitch angle controller is achieving the reference nominal speed ω_β^{ref}. During this control interval, the captured power is constant because the reference torque is maintained at a rated torque of the machine and the rotor speed is controlled to maintain a rated value.

29.2 Power Electronic Converters for Variable Speed Wind Turbines

29.2.1 Introduction

Power electronic converters can operate the stator of synchronous or asynchronous machines. In other applications, the power converter can be connected to the rotor of a wound rotor induction machine. In the first case, the converter handles the overall power of the machine and it operates in a wide speed range. In the wound rotor machine case, the converter handles a fraction of the rated power but it does not allow a very low speed to obtain higher energy from the wind. So, the advantage is that the power converter is smaller and cheaper than the stator converter.

29.2.2 Full Power Conditioner System for Variable Speed Turbines

In this section, the different topologies of power electronic converters that are currently used for wide range speed control of generators will be presented. A variable speed wind turbine control method within a wide range has the following advantage and disadvantage compared to those for narrow-range speed control. The advantage of a variable speed wind turbine control method in a wind range is that it allows for very low speed to obtain higher energy from the wind. On the other hand, the disadvantage is that the power converter must be rated to the 100% of the nominal generation power.

The power conditioners, next to be considered in this section, may be used for synchronous as well as asynchronous generators. For both cases the control block to be employed is defined. The main objective of power converters to be used for wind energy applications is to handle the energy captured from the wind and the injection of this energy into the grid. The characteristics of the generator to be connected to the grid and where to inject the electric energy are decisive when designing the power converter. To attain this design, it is necessary

to consider the type of semiconductor to be used, components and subsystems.

By using cycloconverters (AC/AC) or frequency converters based on double frequency conversion, normally AC/DC–DC/AC, and connected by a DC link, a rapid control of the active and reactive power can be accomplished along with a low incidence in the distribution electric grid. The commutation frequency of the power semiconductors is also an important factor for the control of the wind turbine because it allows not only to maximize the energy captured from the wind but also to improve the quality of the energy injected into the electrical grid. Because of this, the semiconductors required are those that have a high power limit and allow a high commutation frequency. The insulated gate bipolar transistor (IGBTs) are commonly used because of their high breakdown voltage and because they can bear commutation frequencies within the range of 3–25 kHz, depending on the power handled by the device. Other semiconductors such as gate turn-off thyristor (GTOs) are used for high power applications allowing lower commutation frequencies, and thus, worsening not only the control of the generator but also the quality of the energy injected into the electric grid. [4, 8, 9, 10, 18].

The different topologies used for a wide-range rotor speed control are described next. Advantages and disadvantages for using these topologies, as power electronics is concerned, are: Advantages:

- Wide-range speed control
- Simple generator-side converter and control
- Generated power and voltage increased with speed
- VAR-reactive power control possible

Disadvantages:

- One or two full-power converter in series
- Line-side inductance of 10–15% of the generated power
- Power loss up to 2–3% of the generated power
- Large DC link capacitors

29.2.2.1 Double Three Phase Voltage Source Converter Connected by a DC-link

Figure 29.10 shows the scheme of a power condition for a wind turbine. The three phase inverter on the left side of the power converter works as a driver controlling the torque generator by using a vectorial control strategy. The three phase inverter on the right side of the figure permits the injection of the energy extracted from the wind into the grid, allowing a control of the active and reactive power injected into the grid. It also keeps the total harmonic distortion coefficient as low as possible improving the quality of the energy injected into the public grid. The objective of the DC-link is to act as an energy storage, so that the captured energy from the wind is stored as a charge in the capacitors and is instantaneously injected into the grid. The control signal is set to maintain a constant reference to the voltage of the capacitors battery V_{dc}. The control strategy for the connection to the grid will be described in Section 29.2.3.

The power converter shown in Fig. 29.10 can be used for a variable speed control in generators of wind turbines, either for synchronous or asynchronous generators.

29.2.2.1.1 Asynchronous Generator Next to be considered is the case of an asynchronous generator connected to a wind turbine. The control of a variable speed generator requires a torque control, so that for low speed winds the control is required with optimal tip speed ratio, λ_{opt}, to allow maximum captured wind energy from low speed winds. The generator speed is adjusted to the optimal tip speed ratio λ_{opt} by setting a reference speed. For high speed winds the pitch or stall regulation of the blade limits the maximum power generated by the wind turbine. For low winds it is necessary to develop a control strategy, mentioned in Section 29.2.

The adopted control strategy is an algorithm for indirect vector control of an induction machine [3, 6, 7], which is described next and shown in Fig. 29.11.

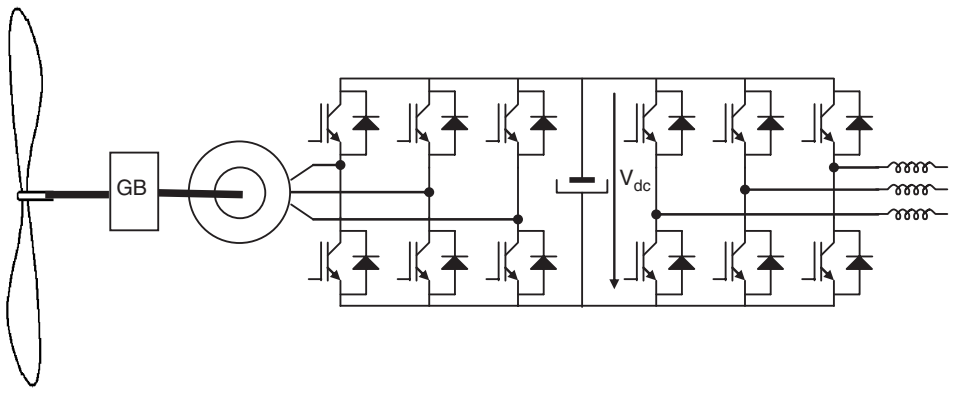

FIGURE 29.10 Double three phase voltage source inverter connected by a DC link used in wind turbine applications.

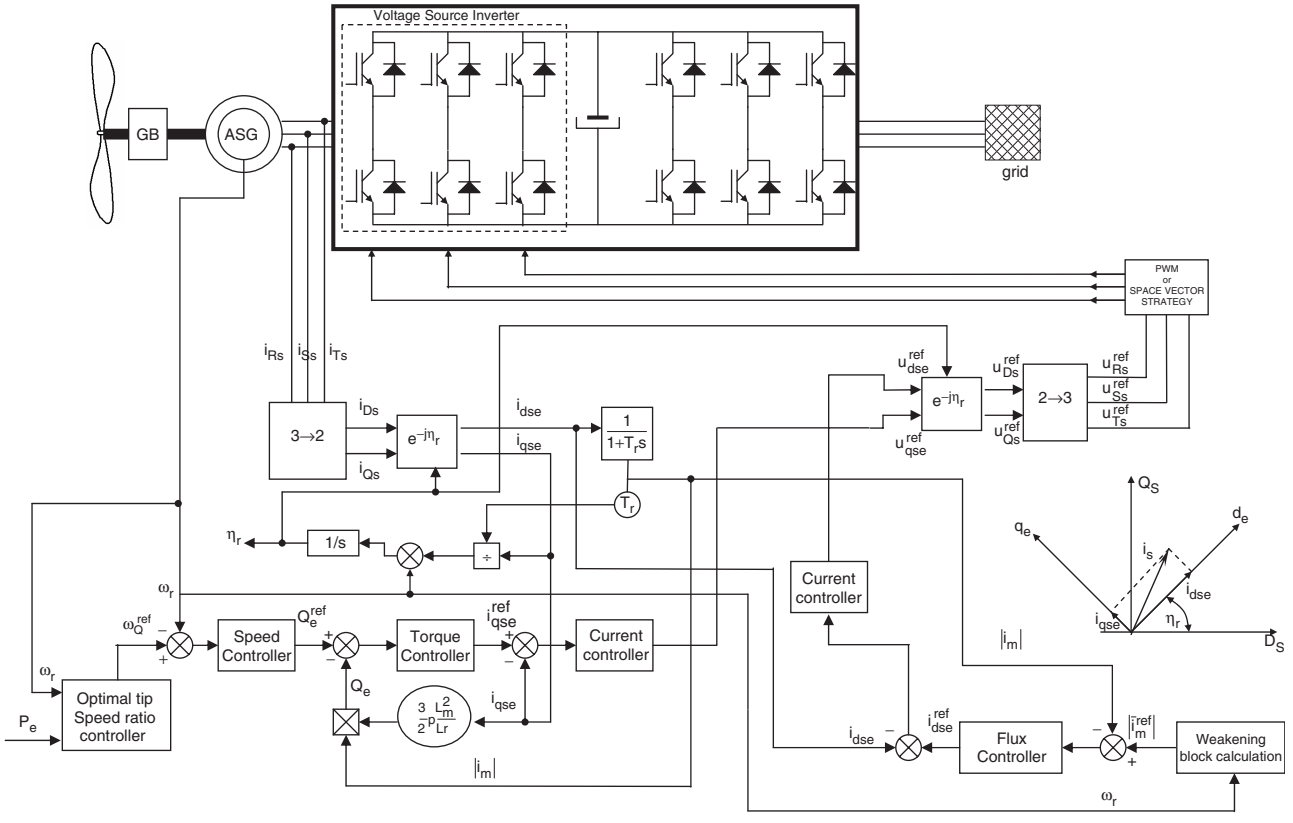

FIGURE 29.11 Schematic of the rotor flux-oriented of a squirrel cage induction generator used in a variable speed wind turbine.

A reference speed, ω_Q^{ref}, has been obtained from the control strategy used in order to achieve optimal speed ratio working conditions of the wind turbine to capture the maximum energy from the wind. In Fig. 29.11, the calculation block to obtain ω_Q^{ref} is shown, that is fed by the actual rotor speed, ω_r, and the electrical power generated, P_e, by the asynchronous generator. Using this ω_Q^{ref} and the actual rotor speed, ω_r, which is measured by the machine, the reference for the electric torque, Q_e^{ref}, is obtained from the speed regulator which is necessary to set the reference torque in the machine shaft in order to achieve the control objectives.

In Fig. 29.11 the induction generator is driven by a voltage-source pulse width moducation (PWM) inverter, which is connected by a second voltage-source PWM inverter to the public grid through a DC link battery capacitors. The output voltage of the inverter is controlled by a PWM technique in order to follow the voltage references, u_{Rs}^{ref}, u_{Ss}^{ref}, u_{Ts}^{ref}, provided by the control algorithm in each phase. There are many types of modulation techniques which are not discussed in detail here.

A flux model has been used to obtain the angular speed of the rotor flux and the modulus of magnetizing current, $|i_m|$, that has also been used to calculate the electromagnetic torque, Q_e, as shown in Fig. 29.11, using the Eq. (29.9).

$$Q_e = \frac{3}{2} \cdot p \cdot \frac{L_m^2}{L_r} \cdot |i_m| \cdot i_{qse} \tag{29.9}$$

The speed controller provides the reference of the torque, Q_e^{ref}, and the torque controller gives the reference value of the quadrature-axis stator current in the rotor flux-oriented reference frame i_{qse}^{ref}.

In Fig. 29.11 the field weakening block, used to obtain the reference value of the modulus of the rotor magnetizing current space phasor $\left|\vec{i}_m^{ref}\right|$, is rotor speed-dependent. This reference signal is then compared with the actual value of the rotor magnetizing current, $|i_m|$, and the error generated is used as input to the flux controller. The output of this controller is the direct-axis stator current reference expressed in the rotor-flux-oriented reference frame i_{dse}^{ref}.

The difference in values of the direct and quadrature-axis stator current references (i_{dse}^{ref}, i_{qse}^{ref}) and their actual values (i_{dse}, i_{qse}) are given as inputs to the respective PI current controllers. The outputs of these PI controllers are values of the direct and quadrature-axis stator voltage reference expressed

in the rotor-flux-oriented reference frame (u_{dse}^{ref}, u_{qse}^{ref}). After this they are transformed into the steady reference frame (u_{Ds}^{ref}, u_{Qs}^{ref}), using the $e^{-j\eta r}$ transformation. This is followed by the 2 → 3 block and finally, the reference values of the three phase stator voltage (u_{Rs}^{ref}, u_{Ss}^{ref}, u_{Ts}^{ref}) are obtained. These signals are used to control the pulse-width modulator, which transforms these reference signals into appropriate on–off switching signals to command the inverter phase.

29.2.2.1.2 Synchronous Generator When the generator, used to transform the mechanical energy into electrical energy in the wind turbine, is a salient-pole synchronous machine with an electrically excited rotor, the control criteria are the same as the one applied in the induction generator case, so as to minimize the angular speed error in order to obtain an optimum tip speed ratio performance of the wind turbine. In this section, a drive control based on magnetizing field-oriented control is described and applied to a wind turbine with a salient-pole synchronous machine. This control method can be applied to the synchronous generator using a voltage-source inverter or a cycloconverter as it is shown in Figs. 29.10 and 29.13 respectively, using the same block control diagram.

In both cases, a controllable three-phase rectifier supplies the excitation winding on the rotor of the synchronous machine. As it is well-known, the cycloconverter is a frequency converter which converts power directly from a fixed frequency to a lower frequency. Each of the motor phases is supplied through a three-phase transformer, an antiparallel thyristor bridge, and the field winding is supplied by another three-phase transformer and a three-phase-rectifier using the bridge connection.

In the control block described in Fig. 29.12, the rotor speed and monitored current have been used in order to control the relationship between the magnetizing flux and currents of the machines by modifying the voltages of the power converter and the excitation current in the field winding.

The reference rotor speed, ω_Q^{ref}, and the measured rotor speed, ω_r, are compared and the error is introduced into the speed controller. The output voltage is proportional to the electromagnetic torque PI, of the synchronous machine and the reference torque, Q_e^{ref}, is obtained. Dividing the reference torque by the modulus of the magnetizing flux-linkage space

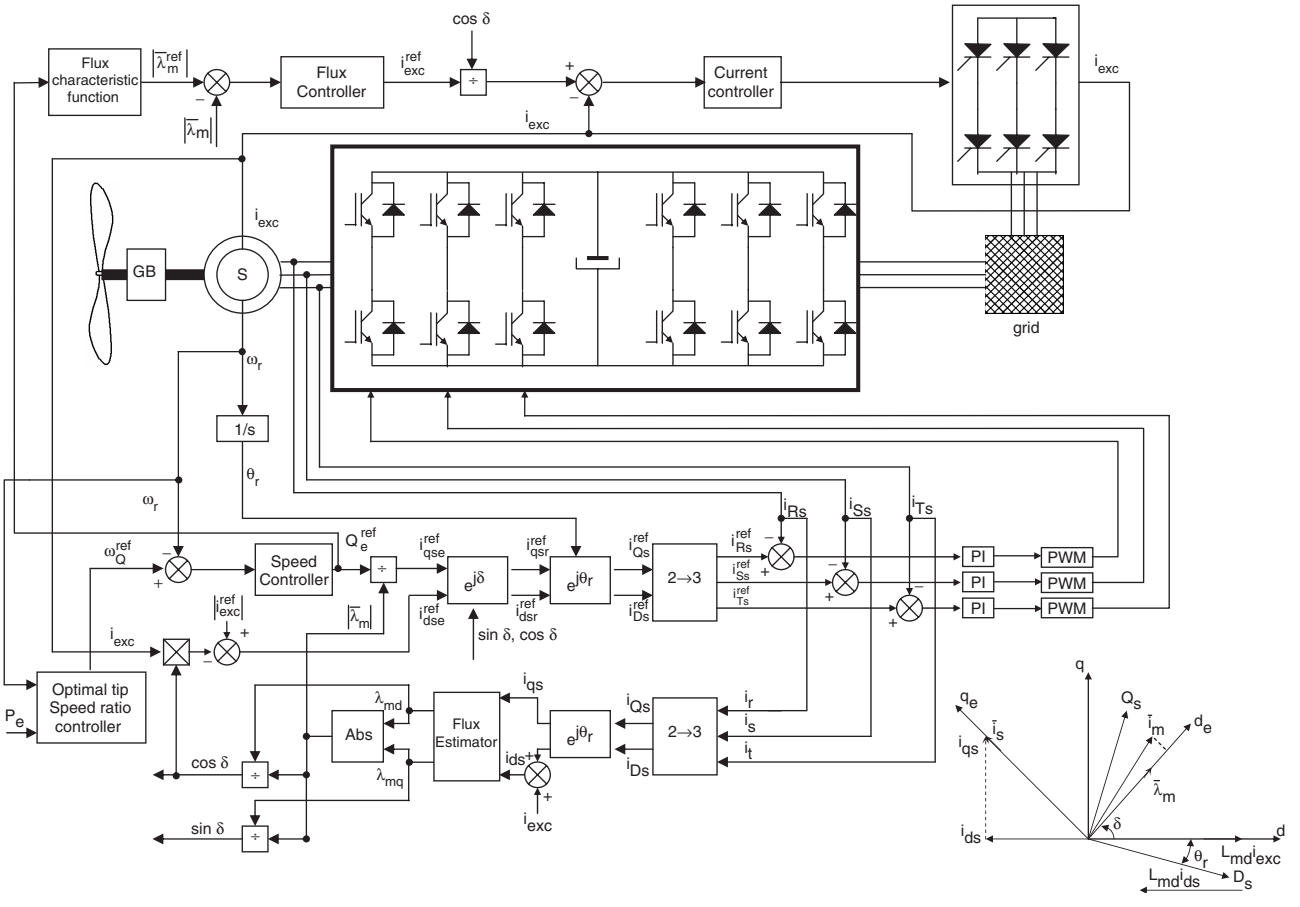

FIGURE 29.12 Block diagram of a field-oriented control of a salient-pole synchronous machine used in wind turbine applications.

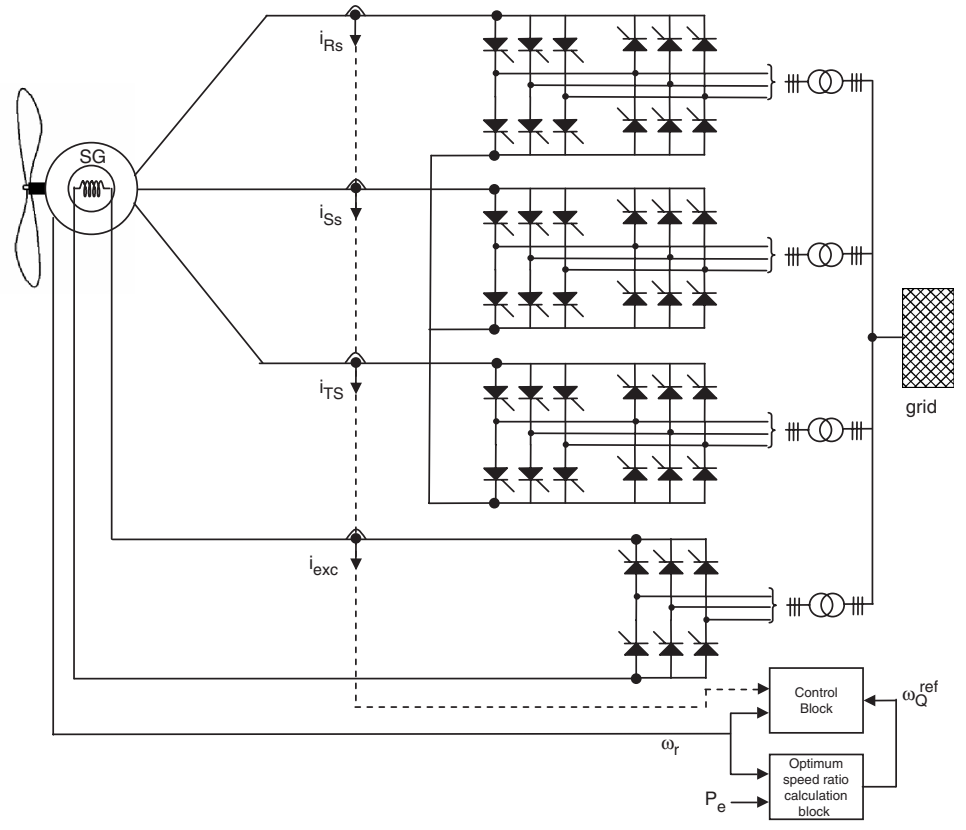

FIGURE 29.13 Schematic of the cycloconverter synchronous generator used in variable speed wind turbines.

phasor $|\lambda_m|$, the reference value of the torque-producing stator current, $|\lambda_m|$, component is obtained.

Using a characteristic function of the magnetizing flux reference and the actual rotor speed, ω_r, the magnetizing flux reference is obtained, $\left|\lambda_m^{ref}\right|$. Below base speed, this function yields a constant value of the magnetizing flux reference, λ_m^{ref}; above base speed, this flux is reduced. The magnetizing flux controller, $\left|\bar{\lambda}_m\right|$, is introduced and compared with the estimated magnetizing flux of the synchronous machine, $\left|\lambda_m^{ref}\right|$, obtaining the error, which is fed into the flux controller as shown in Fig. 29.12. The flux controller maintains the magnetizing linkage flux to a pre-set value independent of the load. As an output of this controller the reference excitation current, i_{exc}^{ref} is obtained.

The value of the reference magnetizing stator current, i_{exc}^{ref}, is obtained using a steady state in which there is no reactive current drawn from the stator [3]. In this case the power factor is unity and the stator current value is the optimal. The zero reactive power condition can be fulfilled by controlling the magnetizing current stator component that is shown in Fig. 29.12.

The stator current components (i_{dsc}^{ref}, i_{qse}^{ref}) are first transformed into the stator current components established in the rotor reference frame (i_{dsr}^{ref}, i_{qsr}^{ref}). After these components are transformed into the stationary-axes current components by a similar transformation, but taking into account that the phase displacement between the stator direct axis of the rotor is θ_r. The obtained two-axis stator current references (i_{Qs}^{ref}, i_{Ds}^{ref}), are transformed into the three phase stator current references (i_{Rs}^{ref}, i_{Ss}^{ref}, i_{Ts}^{ref}) by the application of the three phase to two phase transformation. The reference stator currents are compared with their respective measured currents, and their errors are fed into the respective stator current controllers.

29.2.2.2 Step-up Converter and Full Power Converter

An alternative for the power conditioning system of a wind turbine is to choose a synchronous generator and a three phase diode rectifier, as shown in Fig. 29.14. Such a choice is based on low cost compared with an induction generator connected to a voltage source inverter used as a rectifier. When the speed of the synchronous generator alters, the voltage value on the DC-side of the diode rectifier will change. A step-up chopper is used to adapt the rectifier voltage to the DC-link voltage of the inverter, see Fig. 29.14. When the inverter system is analyzed, the generator/rectifier system can be modeled as an ideal current source. The step-up chopper used as a rectifier utilizes

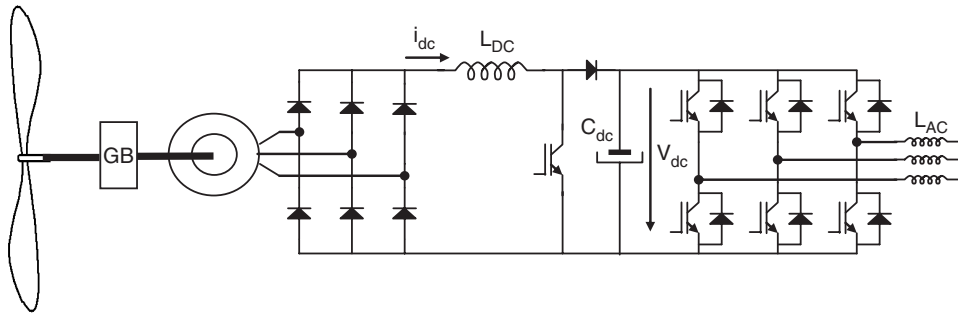

FIGURE 29.14 Step-up converter in the rectifier circuit and full power inverter topology used in wind turbine applications.

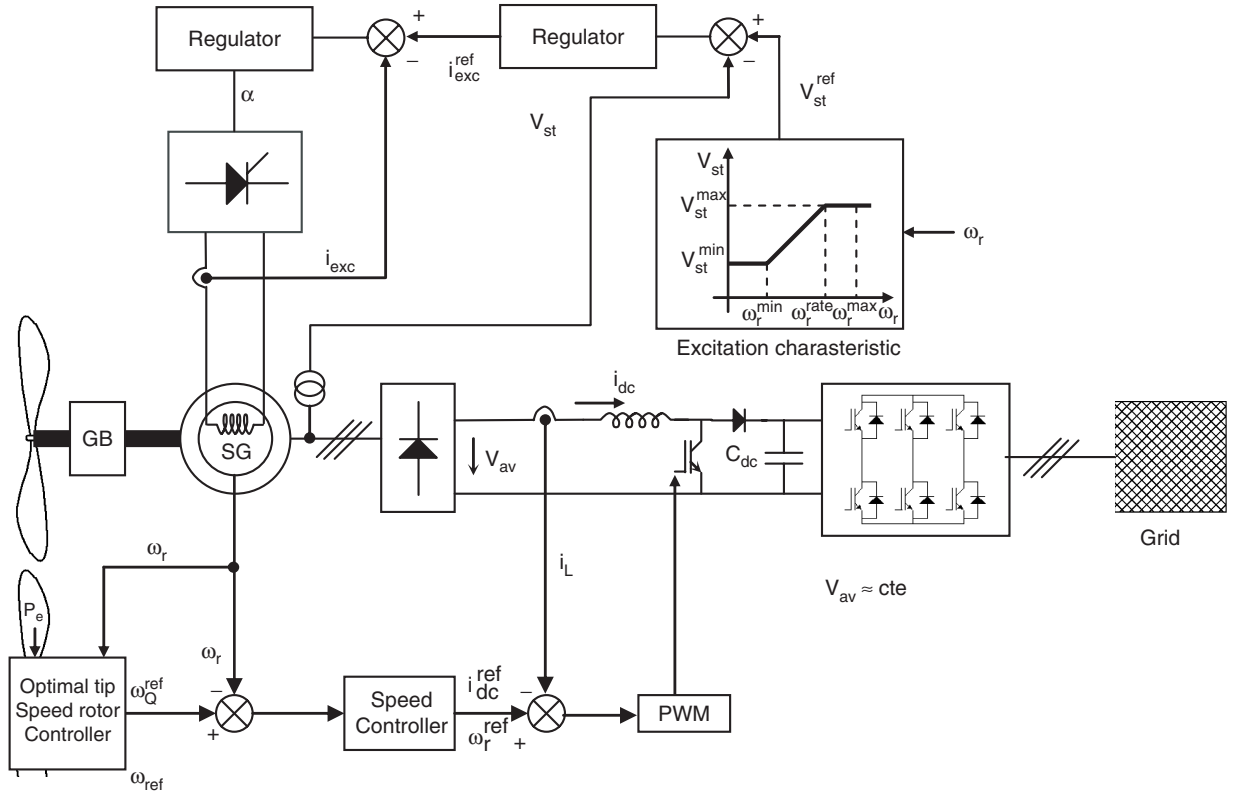

FIGURE 29.15 Control block diagram of a step-up converter in the rectifier circuit and full power inverter used in wind turbine applications.

a high switching frequency so the bandwidth of these components is much higher than the bandwidth of the generator. The generator/rectifier current is denoted as i_{dc} and is independent of the value of the DC-link voltage. The inductor of the step-up converter is denoted as LDC. The capacitor of the DC-link has the value C_{dc}. The inductors on the AC-side of the inverter have the inductance L_{AC}. The three-phase voltage system of the grid has phase voltages e_R, e_S, and e_T and the phase currents are denoted as i_{Rg}, i_{Sg}, and i_{Tg}. The DC-link voltage value is denoted as V_{dc}.

The control system, shown in Fig. 29.15, is based on the measurement of the rotor speed ω_r of the synchronous generator by means of a speed transducer. This value is compared with the reference rotor speed obtained by the control algorithm of the variable speed wind turbine used in the application in order to achieve optimal speed ratio, and therefore, to capture the maximum energy from the wind.

The objective of the synchronous machine excitation system is to keep the stator voltage V_{st} following the excitation characteristic of the generator, shown in Fig. 29.15. This excitation characteristic is linear in the range of the minimum of the rotor speed ω_r^{min} and the rated value of the rotor speed ω_Q^{rate}. Outside this range, the stator voltage is saturated to V_{st}^{min} or V_{st}^{max}. For rotor speeds ω_r in the range between ω_r^{min} and ω_r^{rate}, the

control is carried out using an inductor current i_{dc} proportional to the shaft torque of the generator. Above the rated rotor speed, this current is proportional to the power because the stator voltage V_{st} is constant.

29.2.2.3 Grid Connection Conditioning System

Injection into the public grid is accomplished by means of PWM voltage source interver. This requires the control of the current of each phase of the inverter, as shown in Fig. 29.16. There are several methods of generating the reference current to be injected into any of the phases of the inverter. A very useful method to calculate this current was proposed by Professor Akagi [19], that is applied to the active power filters referred to as "Instantaneous Reactive Power Theory." The control block shown in Fig. 29.16 is based on the comparison of the actual capacitor array voltage V_{dc} with a reference voltage V_{dc}^{ref}. Subtracting the actual capacitor array voltage V_{dc}^{ref} from the reference voltage V_{dc}^{ref}, the error signal voltage is obtained. This error signal is fed into a compensator, usually a PI compensator, that transforms the output to an active instant power signal that, after being injected into the electric grid, is responsible for the error of the regulator of the voltage in the capacitor array to be zero.

Transformation of the phase voltage e_{rg}, e_{sg}, and e_{tg} into the α–β orthogonal coordinates is given by the following expression:

$$\begin{bmatrix} e_\alpha \\ e_\beta \end{bmatrix} = \sqrt{\frac{2}{3}} \cdot \begin{bmatrix} 1 & -1/2 & -1/2 \\ 0 & \sqrt{3}/2 & -\sqrt{3}/2 \end{bmatrix} \cdot \begin{bmatrix} e_{rg} \\ e_{sg} \\ e_{tg} \end{bmatrix} \tag{29.10}$$

Using the inverse transformation equations from the control algorithm [19] and the reference of real power of the capacitor array, it is possible to derive the phase sinusoidal reference current to be injected by the converter into the grid.

$$\begin{bmatrix} i_{rg}^{ref} \\ i_{sg}^{ref} \\ i_{tg}^{ref} \end{bmatrix} = \sqrt{\frac{2}{3}} \cdot \begin{bmatrix} 1 & 0 \\ -1/2 & \sqrt{3}/2 \\ -1/2 & -\sqrt{3}/2 \end{bmatrix} \cdot \begin{bmatrix} e_\alpha & e_\beta \\ -e_\beta & e_\alpha \end{bmatrix}^{-1} \cdot \begin{bmatrix} p^{ref} \\ q^{ref} \end{bmatrix} \tag{29.11}$$

As can be seen in the above equation, the reference of the reactive power appears which is normally set at zero so that the current is being injected into the public grid with unity power factor.

There is another type of wind energy extraction system where the objective is to compensate the reactive power

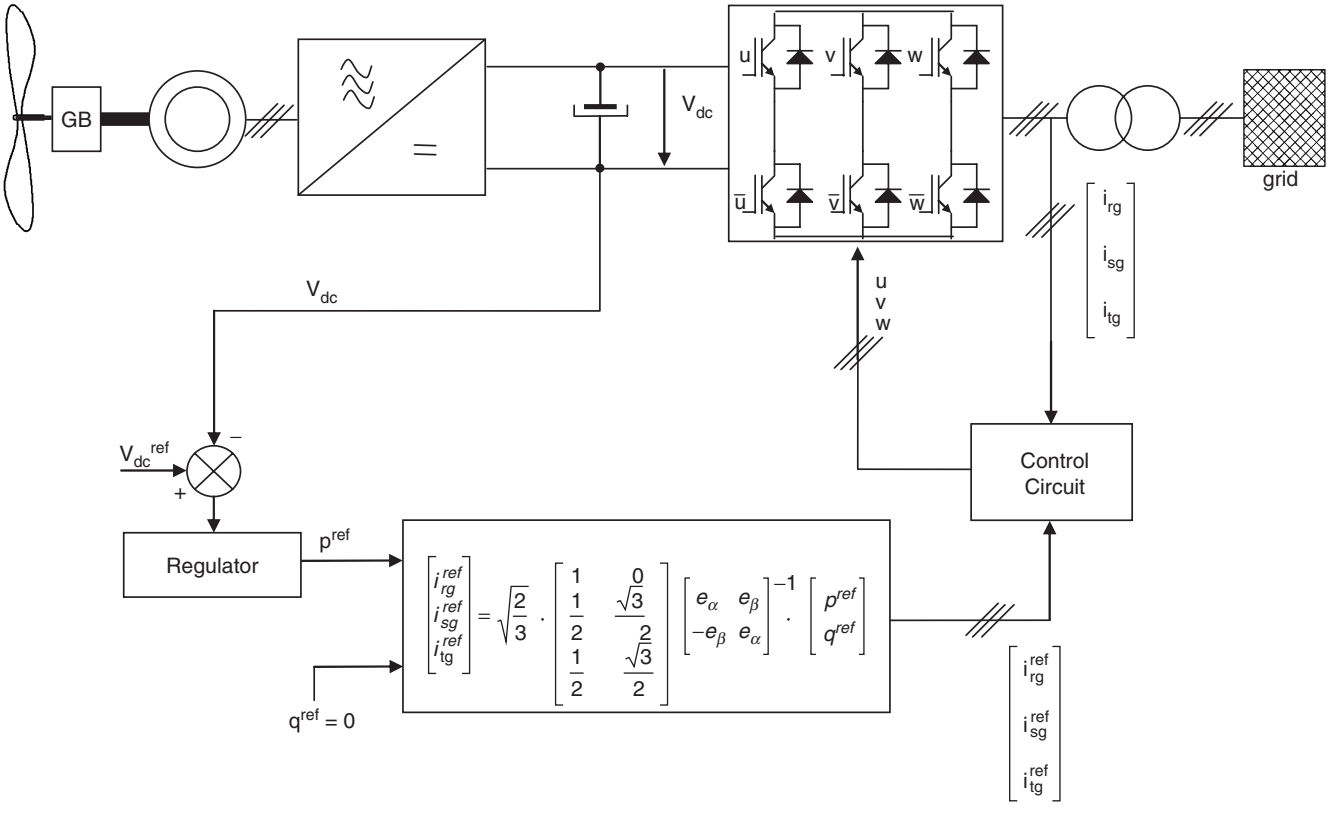

FIGURE 29.16 Control block diagram of the grid connection conditioning system.

generated by non-linear loads of the grid. In this case, the reactive reference power is set to the corresponding value, for either reactive or capacitive power factor "leading or lagging."

29.2.3 Rotor Connected Power Conditioner for Variable Speed Wind Turbines

As it was introduced before, variable speed can also be obtained by slip change of induction generator using a wound rotor machine.

Since it is necessary to have an electric connection to the rotor winding, rotation is achieved by using a slip ring. The power delivered by the rotor through the slip rings is equal to the product of the slip by the electrical power that flows into the stator P_S, Eq. (29.12). This is the so-called "slip power" P_{slip}.

$$P_{slip} = s \cdot P_S \tag{29.12}$$

The slip power can be handled as follows:

- It can be dissipated in a resistor (Fig. 29.17).
- Using a single doubly fed scheme, the slip power is returned to the electrical grid or to the machine stator (Fig. 29.18).
- Using a cascaded scheme. This is accomplished by connecting a second machine. Part of the power is transferred as mechanical power through the shaft, and the other part is transferred to the grid by a power converter (Fig. 29.19).
- A single frame cascaded or brushless doubly fed induction machine [20] can be used in the same way as before, but using only one machine instead of two (Fig. 29.20).

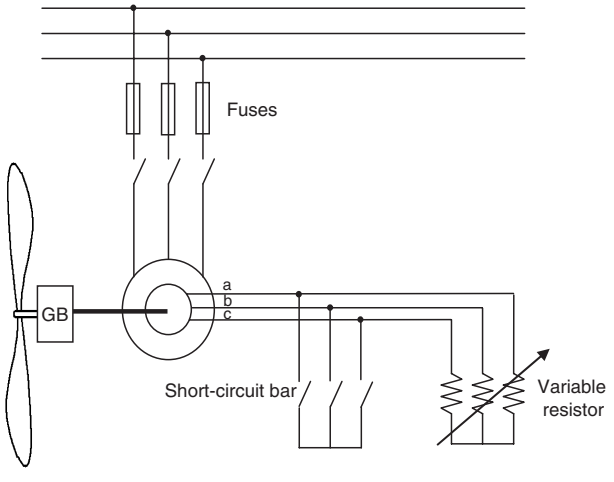

FIGURE 29.17 Slip power dissipation in a resistor.

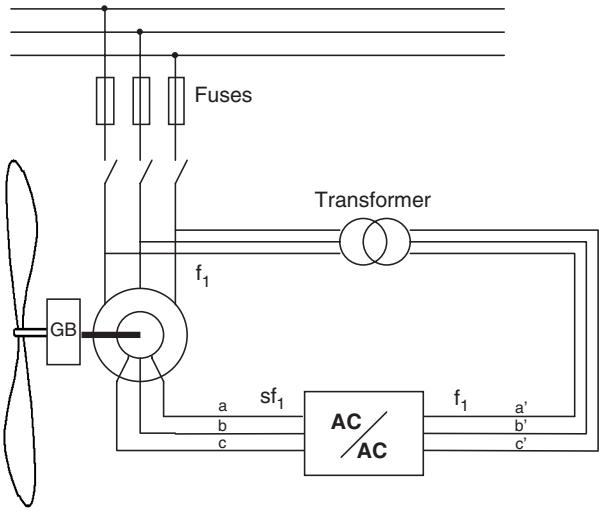

FIGURE 29.18 Single doubly fed induction machine.

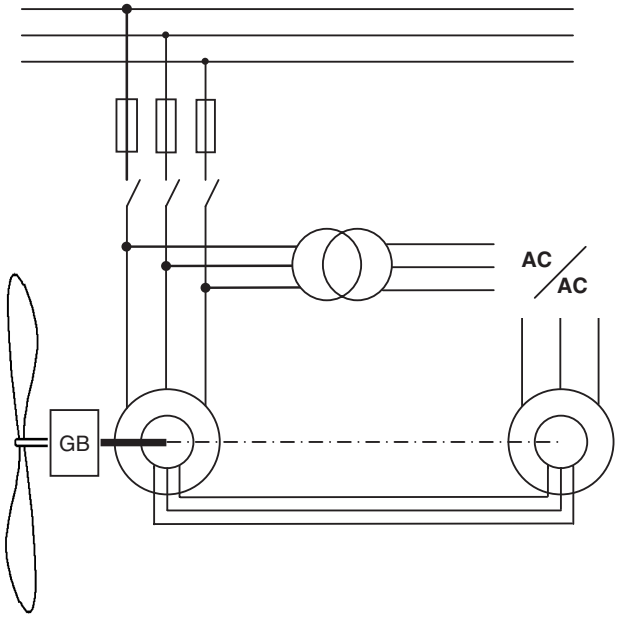

FIGURE 29.19 Wound rotor cascaded induction machines.

29.2.3.1 Slip Power Dissipation

Figure 29.17 shows a system in which the power delivered by the rotor is dissipated in a resistor.

The variable resistor can be substituted by the power converter in Fig. 29.21. The power converter controls the power delivered to the resistor using an uncontrolled rectifier and a parallel DC–DC chopper. This design has the disadvantage of the current having a higher harmonic content. This is caused by the rectangular rotor current waveform in the case of a three phase uncontrolled rectifier. This disadvantage can be avoided using a six IGBT's controlled rectifier, however this topology increases the cost significantly.

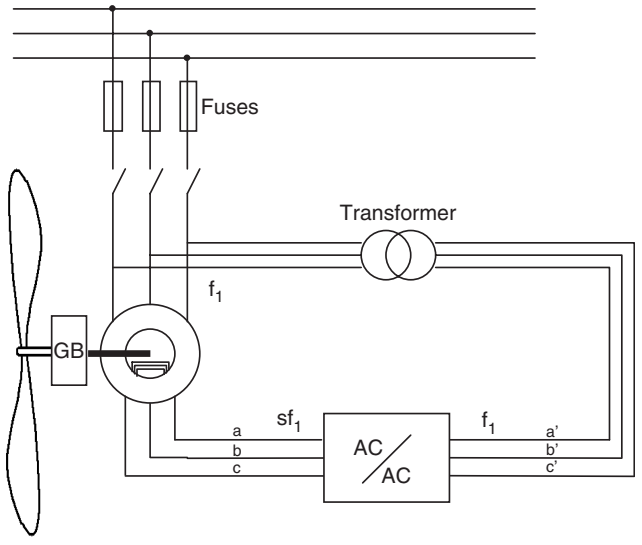

FIGURE 29.20 Brushless doubly fed induction machine.

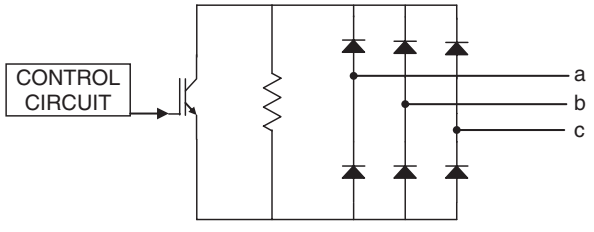

FIGURE 29.21 Variable resistor using a power converter.

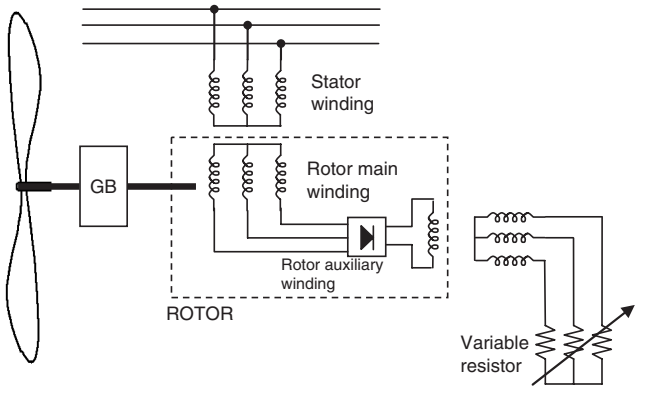

FIGURE 29.22 Slip power dissipation in an external resistor using brushless machine.

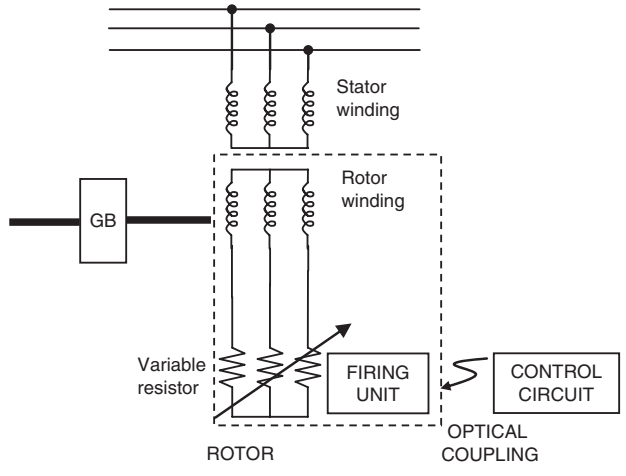

FIGURE 29.23 Slip power dissipation in an internal resistor using brushless machine.

The variation of the rotor resistance is not a recommended technique due to the high copper losses in the regulation resistance and so, the generator system efficiency is lower. It only can be efficient within a very narrow range of the rotor speed. Another disadvantage is that this technique is applicable only to wound-rotor machines and so, slip rings and brushes are needed. In order to solve this problem some brushless schemes are proposed. A solution is to use a rotor auxiliary winding which couples the power to an external variable resistor. The scheme can be observed in Fig. 29.22.

Another solution is to dissipate the energy within a resistor placed in the rotor as it is shown in Fig. 29.23. This method is currently used in generators for wind conversion systems, but as the efficiency of the system decreases with increasing the slip, the speed control is limited to a narrow margin. This scheme includes the power converter and the resistors in the rotor. Trigger signals to the power switches are accomplished by optical coupling.

29.2.3.2 Single Doubly Fed Induction Machine

In Fig. 29.18 the connection scheme shows that slip power is injected into the public grid by a power converter and a transformer. The power converter changes the frequency and controls the slip power. In some cases a transformer is used due to public grid voltages which can be higher than rotor voltages.

Disregarding losses, the simplified scheme of Fig. 29.24 shows real power flux in all different connection points of the diagram. In this figure, the electrical power in the stator machine P_S, the mechanical power $(1 - s) \cdot P_S$, and the slip power and power converter $s \cdot P_S$ are represented.

In generation mode, the power is positive when the arrow direction shown in Fig. 29.24 is considered. The power handled on the power converter depends on the sign of the machine slip. When this slip is positive, i.e. subsynchronous mode of operation, the slip power goes through the converter from the grid to the rotor of the machine. On the other hand, when the slip is negative, i.e. hypersynchronous mode of operation, the slip power comes out of the rotor to the power converter. Since the slip power is the real power through the converter, this power is determined directly by the maximum slip or by the speed range of the machine. For instance, if the speed range

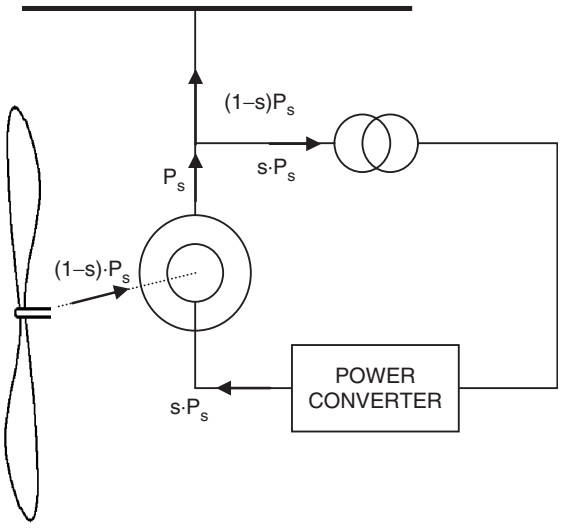

FIGURE 29.24 Simplified scheme of a single doubly fed induction machine.

used is 20% of the synchronous speed, the power rating of the converter is 20% of the main power.

29.2.3.3 Power Converter in Wound-rotor Machines

The power converter used in wound-rotor machines can be a force-commutated converter connected to a line-commutated converter by an inductor as shown in Fig. 29.25. In this case, the power can only flow from the rotor to the grid, and the induction generator works above synchronous speed. Main disadvantages of this scheme are a low power factor and a high content of low frequency harmonics whose frequency depends on the speed.

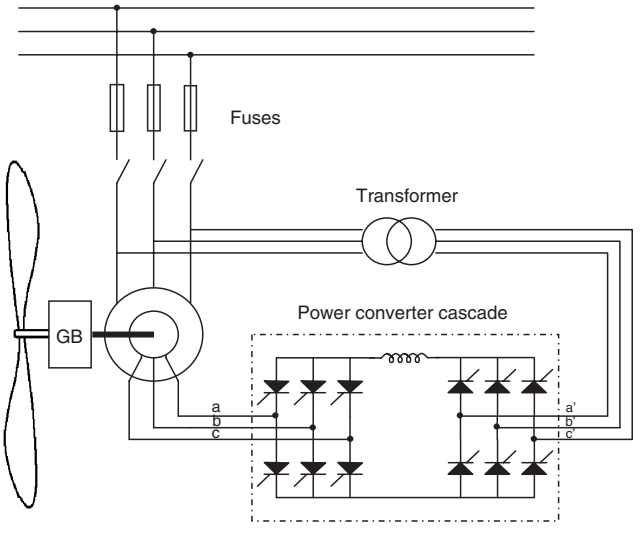

FIGURE 29.25 Single doubly fed induction machine with a force-commutated converter connected to a line-commutated converter.

Since the feeding frequency of the rotor is much lower than the grid's, a cycloconverter, as shown in Fig. 29.26, can be used. In this case the controllability of the system is greatly improved. The cycloconverter is an AC–AC converter based on the use of two three-phase thyristor bridges connected in parallel, one for each phase. This scheme allows working with speed above and below the synchronous speed.

The two schemes mentioned before (Figs. 29.25 and Fig. 29.26) are based on line switched converters. A disadvantage of this scheme is that voltages in the rotor decrease when the machine is working in frequencies close to the synchronous frequency. This fact makes the line-commutated converter not to commute satisfactorily, and we need to use a forced-commutated converter. Also, when a forced-switched converter is used, quality of the voltage and current injected into the public grid is improved. The forced-switched power converter scheme is shown in Fig. 29.27. The converter includes two three-phase AC–DC converters linked by a DC capacitor battery. This scheme allows, on one hand, a vector control of the active and reactive power of the machine, and on the other hand, a decrease by a high percentage of the harmonic content injected into the grid by the power converter.

29.2.3.4 Control of Wound-rotor Machines

The vector control of the rotor flux can be accomplished very easily in a wound-rotor machine. Power converters that can be used for vector control applications are either a controlled rectifier in series with an inverter or a cycloconverter.

In this system, the slip power can flow in both directions, from the rotor to the grid (subsynchronous) or from the grid to the rotor (hyper-synchronous). In both working modes, the machine must be working as a generator. When the speed is hyper-synchronous, the converter connected to the rotor will work as a rectifier and the converter connected to the grid as an inverter, as was deduced before from Fig. 29.24.

The wound-rotor induction machine can be modeled as follows (see nomenclature page):

$$u_S = R_S \cdot i_S + \frac{d\lambda_S}{dt} \tag{29.13}$$

$$u'_r = n^2 \cdot R_r \cdot i'_r + \frac{d\lambda'_r}{dt} - j \cdot \omega_r \cdot \lambda'_r \tag{29.14}$$

$$\lambda_S = L_S \cdot i_S + n \cdot L_m \cdot i'_r \tag{29.15}$$

$$\lambda'_r = n^2 \cdot L_S \cdot i'_r + n \cdot L_m \cdot i_S \tag{29.16}$$

$$Q_e = \frac{3}{2} \cdot \frac{\rho}{2} \cdot I_m \left\{ \lambda_r \cdot i_r^* \right\} \tag{29.17}$$

$$P_S = \frac{3}{2} \cdot R_e \left\{ u_S \cdot i_s^* \right\} \tag{29.18}$$

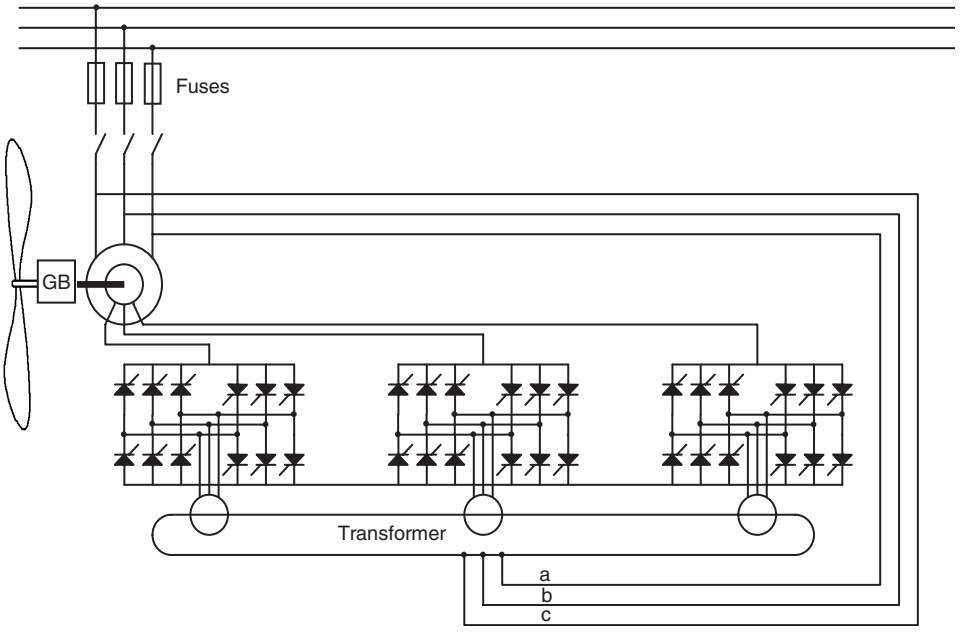

FIGURE 29.26 Single doubly fed induction machine with a cycloconverter.

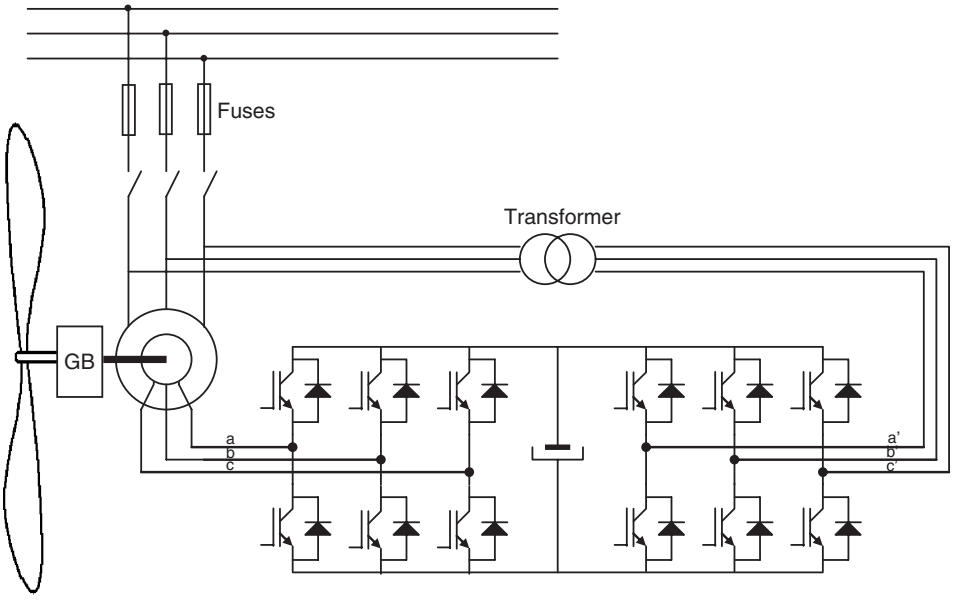

FIGURE 29.27 Single doubly fed induction machine with two fully controlled AC–DC power converters.

$$Q_S = \frac{3}{2} \cdot I_m \left\{ u_S \cdot i_S^* \right\} \tag{29.19}$$

In the induction machine model, rotor magnitudes, the rotor voltage u_r, the rotor flux λ_r, and the rotor current i_r are referred to the stator, and so, the rotor voltage u_r', the rotor flux λ_r', and the rotor current i_r' are defined as:

$$u_r' = n \cdot u_r \cdot e^{j \cdot \theta_r} \tag{29.20}$$

$$\lambda_r' = n \cdot \lambda_r \cdot e^{j \cdot \theta_r} \tag{29.21}$$

$$i_r' = \frac{i_r \cdot e^{j \cdot \theta_r}}{n} \tag{29.22}$$

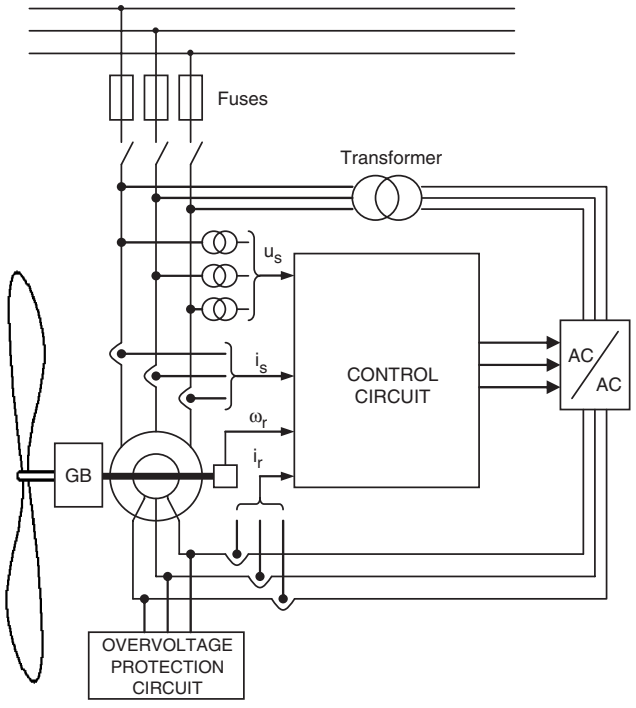

FIGURE 29.28 Wind turbine control block.

The stator magnetizing current i_m is defined as:

$$i_m = \frac{\lambda_S}{n \cdot L_m} = \frac{L_S}{n \cdot L_m} \cdot i_S + i_r' \tag{29.23}$$

Figure 29.28 shows the control block of a wound-rotor induction machine. The wound-rotor induction machine is controlled by the rotor using a power converter that controls the rotor current i_r' by changing the rotor voltage u_r'. The control of the stator current via the rotor current makes sense only if the converter power is kept lower than the rated power of the machine. The AC stator voltage generates a rotating magnetic field with angular frequency ω_e. Relative to the rotor, this magnetic field rotates only with the angular slip frequency. The frequency of voltages induced in the rotor is low, so voltages of the power converter are low too. Active and reactive power of the induction generator, or a certain percentage of them, can be controlled by the rotor current.

The machine model can be referred to the reference axes that move with the magnetizing current. This system of coordinates rotates with an angle θ_e relative to the stator. In these axes $i_{qm} = 0$ as shown in Fig. 29.29.

Equations of the rotor and stator voltage become:

$$u_S = R_S \cdot i_S + \frac{d\lambda_S}{dt} + j \cdot \omega_e \cdot \lambda_S \tag{29.24}$$

$$u_r' = n^2 \cdot R_r \cdot i_r' + \frac{d\lambda_r'}{dt} + j \cdot (\omega_e - \omega_r) \cdot \lambda_r' \tag{29.25}$$

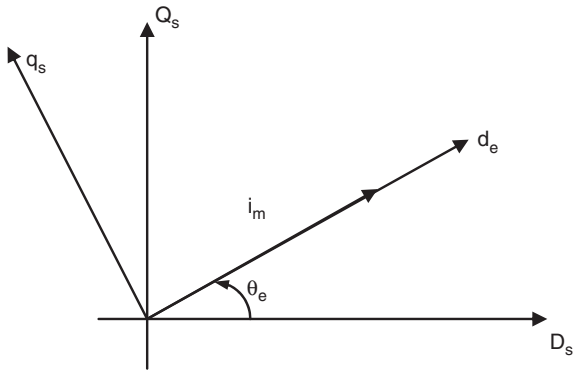

FIGURE 29.29 Stator and rotor reference frames.

$$\omega_e = \frac{d\theta_e}{dt} \tag{29.26}$$

Supposing steady-state conditions and disregarding the resistors in the stator and the rotor, because the voltage drop is very low in comparison to the stator voltage, the stator and rotor voltages can be determined as:

$$u_S = j\omega_e \lambda_S \tag{29.27}$$

$$u_r' = j\omega_{s1} \lambda_r' \tag{29.28}$$

The flux is determined from the stator voltage u_S and the angular frequency ω_e of the AC system. Since both are constant, the flux linkage and magnetizing current are constant too.

$$i_m = \frac{\lambda_S}{nL_m} = \frac{u_{ds} + ju_{qs}}{j\omega_e nL_m} \tag{29.29}$$

As i_m is constant, the stator current can be controlled at any time, by means of controlling the rotor current that can be deduced from Eq. (29.23). From Eq. (29.29) we can also deduce that the direct component of the stator voltage u_{ds} is zero due to the quadrature component of the stator magnetizing current i_{qm} is zero and so, the active and reactive power can be obtained by the following equations:

$$P_S = \frac{3}{2} u_{ds} i_{dsm} \tag{29.30}$$

$$Q_S = \frac{3}{2} u_{qs} i_{qsm} \tag{29.31}$$

Figure 29.30 shows a block diagram of a vector control of active and reactive power for a wound-rotor machine. Vector control of cascaded doubly fed machine is presented in [21].

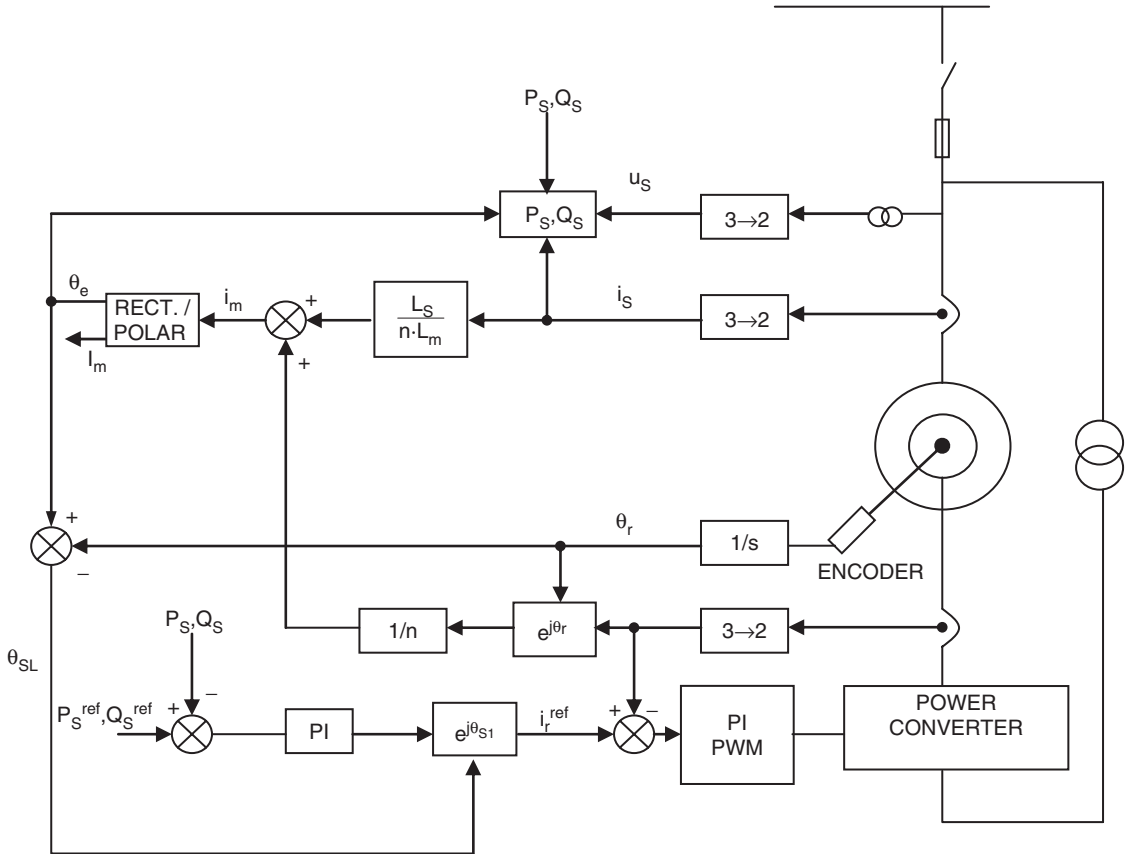

FIGURE 29.30 Power control diagram of the wound-rotor machine.

29.2.4 Grid Connection Standards for Wind Farms

29.2.4.1 Voltage Dip Ride-through Capability of Wind Turbines

As wind capacity increases, network operators have to ensure that consumer power quality is not compromised. To enable large-scale application of wind energy without compromising power system stability, the turbines should stay connected and contribute to the grid in case of a disturbance such as a voltage dip. Wind farms should generate similar to conventional power plants supplying active and reactive power for frequency and voltage recovery, immediately after the fault has been produced.

Thus, several utilities have introduced special grid connection codes for wind farm developers, covering reactive power control, frequency response, and fault ride-through, especially in places where wind turbines provide for a significant part of the total power. Examples are Spain [22], Denmark [23], and part of Northern Germany [24].

The correct interpretation of these codes is crucial for wind farm developers, manufacturers, and network operators. They define the operational boundary of a wind turbine connected to the network in terms of frequency range, voltage tolerance, power factor, and fault ride-through. Among all these requirements, fault ride-through is regarded as the main challenge to the wind turbine manufacturers. Though the definition of fault ride-through varies, the E.ON (German Transmission and Distribution Utility) regulation is likely to set the standard [24]. This stipulates that a wind turbine should remain stable and connected during the fault, while voltage at the point of connection drops to 15% of nominal (i.e. a drop of 85%) for a period of 150 ms: see Fig. 29.31.

Only when the grid voltage drops below the curve, the turbine is allowed to disconnect from the grid. When the voltage is in the shaded area, the turbine should also supply reactive power to the grid in order to support grid voltage restoration.

A major drawback of variable-speed wind turbines, especially for turbines with doubly fed induction generators (DFIGs), is their operation during grid faults [25, 26]. Faults in the power system, even far away from the location of the turbine, can cause a voltage dip at the connection point of the wind turbine. The dip in the grid voltage will result in an increase of the current in the stator windings of the DFIG. Because of the magnetic coupling between the stator

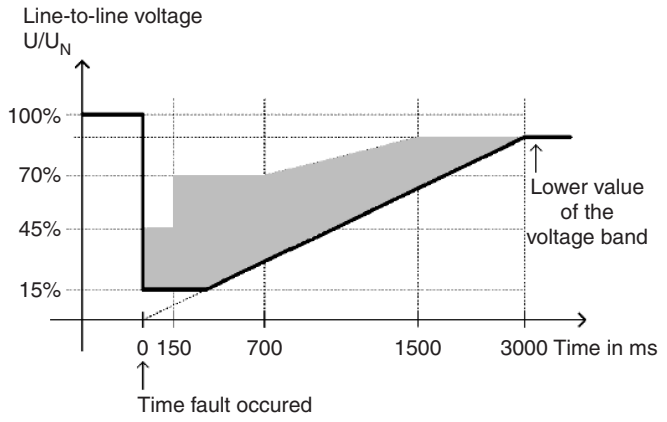

FIGURE 29.31 E. On Netz requirements for wind farm behavior during faults.

and rotor, this current will also flow in the rotor circuit and the power electronic converter. This can lead to the permanent damage of the converter. It is possible to try to limit the current by current-control on the rotor side of the converter; however, this will lead to high voltages at the converter terminals, which might also lead to the destruction of the converter. A possible solution that is sometimes used is to short-circuit the rotor windings of the generator with the so-called crowbars.

The key of the protection technique is to limit the high currents and to provide a bypass for it in the rotor circuit via a set of resistors that are connected to the rotor windings (Fig. 29.32). This should be done without disconnecting the converter from the rotor or from the grid. Thyristors can be used to connect the resistors to the rotor circuit. Because the generator and converter stay connected, the synchronism of operation remains established during and after the fault. The impedance of the bypass resistors is of importance but not critical. They should be sufficiently low to avoid excess voltage on the converter terminals. On the other hand, they should be high enough to limit the current. A range of values can be found that satisfies both conditions. When the fault in the grid is cleared, the wind turbine is still connected to the grid. The resistors can be disconnected by inhibiting the gating signals and the generator resumes normal operation.

29.2.4.2 Power Quality Requirements for Grid-connected Wind Turbines

The grid interaction and grid impact of wind turbines has been focused in the past few years. The reason behind this interest is that wind turbines are among utilities considered to be potential sources of bad power quality. Measurements show that the power quality impact of wind turbines has been improved in recent years. Especially variable-speed wind turbines have some advantages concerning flicker. But a new problem is faced with variable-speed wind turbines. Modern forced-commutated inverters used in variable-speed wind turbines produce not only harmonics but also inter-harmonics.

The IEC initiated the standardization on power quality for wind turbines in 1995 as a part of the wind turbine standardization in TC88. In 1998, the IEC issued a draft IEC-61400-21 standard for "Power Quality Requirements for Grid Connected Wind Turbines" [27]. The methodology of that IEC standard consists on three analyses. The first one is the flicker analysis. IEC-61400-21 specifies a method that uses current and voltage time series measured at the wind turbine terminals to simulate the voltage fluctuations on a fictitious grid with no source of voltage fluctuations other than the wind turbine switching operation. The second one is switching operations.

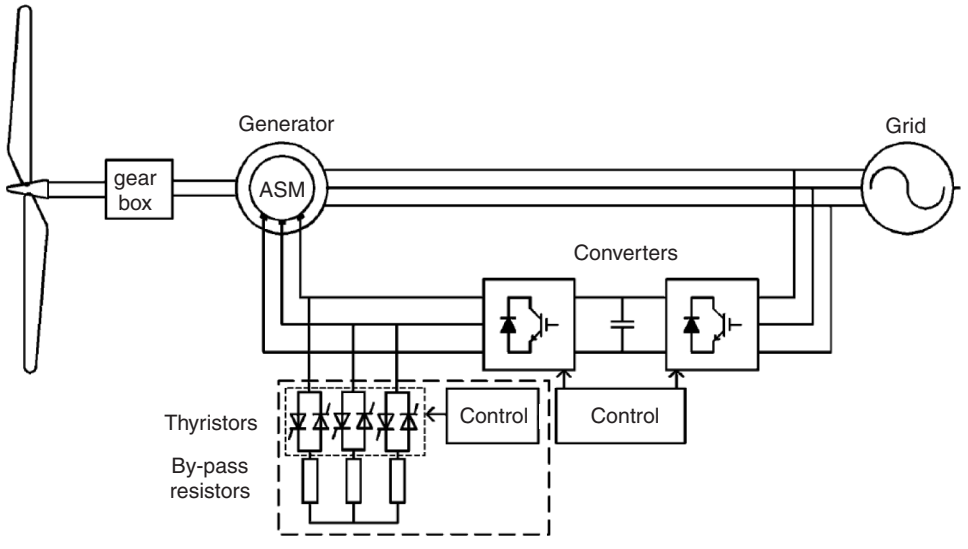

FIGURE 29.32 DFIG bypass resistors in the rotor circuit.

Voltage and current transients are measured during the switching operations of the wind turbine (start-up at cut wind speed and start-up at rated wind speed). The last one is the harmonic analysis which is carried out by the fast fourier transform (FFT) algorithm. Rectangular windows of eight cycles of fundamental frequency width, with no gap and no overlapping between successive windows are applied. Furthermore, the current total harmonic distortion (THD) is calculated up to 50th harmonic order [28, 29].

Recently, high frequency harmonics and inter-harmonics are treated in the IEC 61000-4-7 and IEC 61000-3-6 [30, 31]. The methods for summing harmonics and inter-harmonics in the IECE61000-3-6 are applicable to wind turbines. In order to obtain a correct magnitude of the frequency components, the use of a well-defined window width, according to the IEC 61000-4-7, Amendment 1 is of a great importance, as it has been reported in ref. [32]

Wind turbines not only produce harmonics, they also produce inter-harmonics, i.e. harmonics which are not a multiple of 50 Hz. Since the switching frequency of the inverter is not constant but varies, the harmonics will also vary. Consequently, since the switching frequency is arbitrary, the harmonics are also arbitrary. Sometimes they are a multiple of 50 Hz and sometimes they are not. Figure 29.33 shows the total harmonics spectrum from a variable-speed wind turbine. As can be seen in the figure, at lower frequencies there are only pure harmonics but at higher frequencies there are a whole range of harmonics and inter-harmonics. This whole range of harmonics and inter-harmonics represents variations in the switching frequency of that wind turbine.

29.3 Multilevel Converter for Very High Power Wind Turbines

29.3.1 Multilevel Topologies

In 1980s, power electronics concerns were focused on the increase of the power converters by increasing the voltage or current to fulfill the requirements of the emerging applications. There were technological drawbacks, that endure nowadays, which make impossible to increase the voltage or current in the individual power devices, so researchers were developing new topologies based on series and parallel association of individual power devices in order to manage higher levels of current and voltage, respectively. Due to the higher number of individual power devices on such topologies it is possible to obtain more than the classical two levels of voltage at the output of the converter hence the multilevel denomination for this converter.

29.3.2 Diode Clamp Converter (DCC)

In 1981, Nabae *et al.* presented a new neutral-point-clamped PWM inverter (NPC-PWM) [33]. This converter was based on a modification of the two-level converter topology. In the two-level case, each power switch must support at the most a voltage equal to DC-link total voltage so the switches should be dimensioned to support such voltage.

The proposed modification adds two new switches and two clamp diodes in each phase. In this converter each transistor support at the most a half of the total DC-link voltage; hence,

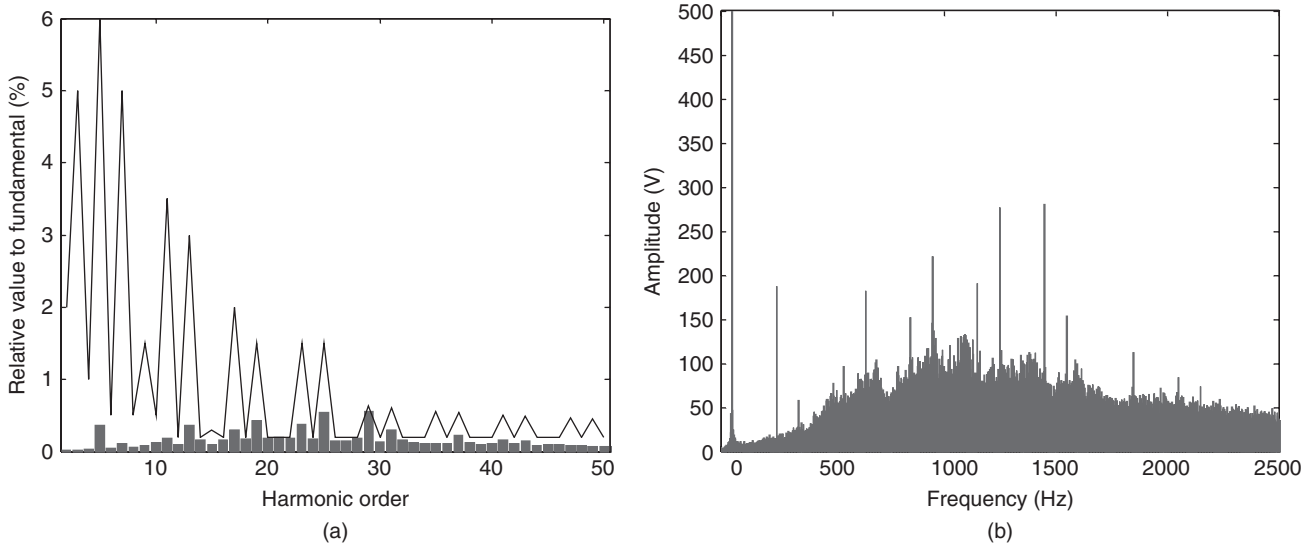

FIGURE 29.33 Typical results of a variable-speed wind turbine with a synchronous generator and full converter. (a) Harmonic content and the comparison with the maximum level of IEC 1000-3-6 standard and (b) harmonic and inter-harmonic content in voltage.

if the used power devices have the same characteristics of those used in the two-level case, the DC-link can be doubled and hence, the power which the converter can manage. Figure 29.34 shows one phase of a three-level DCC with the capacitors voltage divider and the additional switches and diodes.

The analysis of the DCC converter states shows that there are three different switching configurations. These possible configurations are shown in Table 29.1.

When transistors S_3 and S_4 are switched on, the phase is connected to the lowest voltage in the DC-link. In the same manner, when the transistors S_1 and S_2 are switched on, the phase is connected to the highest voltage in the DC-link, and when the transistors S_2 and S_3 are switched on, the phase is connected to the mid DC-link voltage through one of the transistors and clamping diodes.

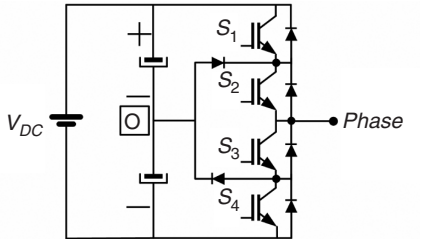

FIGURE 29.34 Three-level DCC.

TABLE 29.1 Switching configurations for the three-level DCC

State	S_1	S_2	S_3	S_4	Phase-O voltage
0	Off	Off	On	On	$-V_{DC}/2$
1	Off	On	On	Off	0
2	On	On	Off	Off	$V_{DC}/2$

29.3.3 Full Converter for Wind Turbine Based on Multilevel Topology

In order to decrease the cost per megawatt and to increase the efficiency of the wind energy conversion, the nominal power of wind turbines has been continuously growing in the last years. The limitations of the two-level converters power ratings versus three-level ones and the capacity of this to reduce the harmonic distortion and electromagnetic interferences (EMI) make the multilevel converters suitable for modern high power wind turbine applications.

Figure 29.35 shows the diagram of high power wind turbine directly connected to the utility grid, with a full converter based on two coupled three-level DCC. The converter connected to the generator acts like an AC–DC converter and its main function is to extract the energy from the generator and to deliver it to the DC-link. The converter connected to the grid acts like a DC–AC converter and its main function is to collect the energy at the DC-link and to deliver it to the utility grid.

29.3.4 Modeling

The use of multilevel converters is limited by the following drawbacks: typically very complex, control and voltage imbalance problems at the DC-link capacitors. An analytical model of the whole system is necessary to study this dynamic and to develop control algorithms that meet with the design specifications.

In [34], a general modeling strategy is proposed to obtain the equations that describe the dynamics of the currents and the capacitors voltages as functions of the control signals that represent the voltage in each phase. Based on the nomenclature that can be seen in Fig. 29.36, this modeling strategy yields in the next mathematical model for the currents dynamics Eqs. (29.32), (29.33):

$$\begin{bmatrix} v_{sr1} \\ v_{sr2} \\ v_{sr3} \end{bmatrix} = L_r \begin{bmatrix} di_{r1}/dt \\ di_{r2}/dt \\ di_{r3}/dt \end{bmatrix} + \frac{1}{3} \begin{bmatrix} 2 & -1 & -1 \\ -1 & 2 & -1 \\ -1 & -1 & 2 \end{bmatrix} \begin{bmatrix} v_{r1} \\ v_{r2} \\ v_{r3} \end{bmatrix} \quad (29.32)$$

$$\begin{bmatrix} v_{si1} \\ v_{si2} \\ v_{si3} \end{bmatrix} = -L_i \begin{bmatrix} di_{i1}/dt \\ di_{i2}/dt \\ di_{i3}/dt \end{bmatrix} + \frac{1}{3} \begin{bmatrix} 2 & -1 & -1 \\ -1 & 2 & -1 \\ -1 & -1 & 2 \end{bmatrix} \begin{bmatrix} v_{i1} \\ v_{i2} \\ v_{i3} \end{bmatrix} \quad (29.33)$$

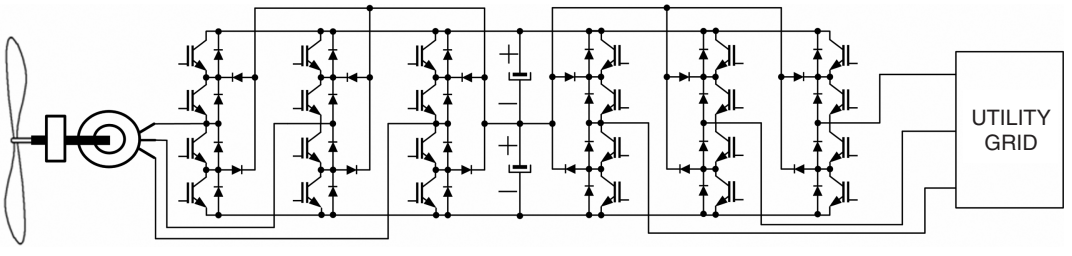

FIGURE 29.35 Diagram of a high power wind turbine with a full converter directly connected to the utility grid.

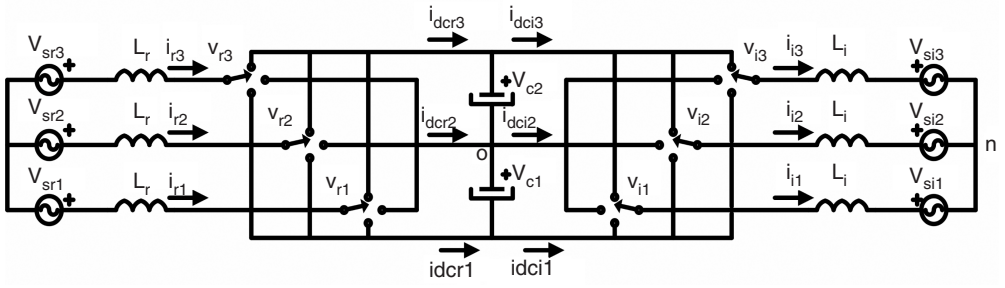

FIGURE 29.36 Nomenclature criterion for the modeling of the full DCC converter.

And the next ones for capacitors voltages dynamics Eq. (29.34):

$$
\begin{aligned}
2C\frac{dx_1}{dt} &= (\delta_{r1}i_{r1} + \delta_{r2}i_{r2} + \delta_{r3}i_{r3}) - (\delta_{i1}i_{i1} + \delta_{i2}i_{i2} + \delta_{i3}i_{i3}) \\
x_1 &= \frac{v_{c1} + v_{c2}}{2} \\
2C\frac{dx_2}{dt} &= \left(\delta_{r1}^2 i_{r1} + \delta_{r2}^2 i_{r2} + \delta_{r3}^2 i_{r3}\right) - \left(\delta_{i1}^2 i_{i1} + \delta_{i2}^2 i_{i2} + \delta_{i3}^2 i_{i3}\right) \\
x_2 &= \frac{v_{c2} - v_{c1}}{2}
\end{aligned}
\tag{29.34}
$$

where, x_1 and x_2 are chosen as variables to facilitate the controller design and represent the dynamics of the sum and the difference of the capacitors voltages, respectively.

As indicated in [34], it is useful to represent the system in $\alpha\beta\gamma$-coordinates because after the transformation appears the γ control signal as a third freedom degree of the control, moreover this transformation shows the direct relation between this control signal and the capacitors voltage balance. To change to the $\alpha\beta\gamma$-coordinates, an invariant power transformation has been used. The voltages and currents, which are vectors originally in *abc*-coordinates, are transformed into $\alpha\beta\gamma$-coordinates according to the following matrix transformation shown in Eq. (29.35):

$$
T = \sqrt{\frac{2}{3}}\begin{bmatrix} 1 & -1/2 & -1/2 \\ 0 & \sqrt{3}/2 & -\sqrt{3}/2 \\ 1/\sqrt{2} & 1/\sqrt{2} & 1/\sqrt{2} \end{bmatrix} \tag{29.35}
$$

The transformed equations are:

$$
\begin{aligned}
L_r\begin{bmatrix} \dfrac{di_{r\alpha}}{dt} \\ \dfrac{di_{r\beta}}{dt} \end{bmatrix} &= \begin{bmatrix} v_{sr\alpha} \\ v_{sr\beta} \end{bmatrix} - x_1\begin{bmatrix} \delta_{r\alpha} \\ \delta_{r\beta} \end{bmatrix} \\
&\quad - x_2\begin{bmatrix} \dfrac{\delta_{r\alpha}^2 - \delta_{r\beta}^2}{\sqrt{6}} + \dfrac{2\delta_{r\alpha}\delta_{r\gamma}}{\sqrt{3}} \\ -\sqrt{\frac{2}{3}}\delta_{r\alpha}\delta_{r\beta} + \frac{2}{\sqrt{3}}\delta_{r\beta}\delta_{r\gamma} \end{bmatrix}
\end{aligned}
\tag{29.36}
$$

$$
\begin{aligned}
L_i\begin{bmatrix} \dfrac{di_{i\alpha}}{dt} \\ \dfrac{di_{i\beta}}{dt} \end{bmatrix} &= -\begin{bmatrix} v_{si\alpha} \\ v_{si\beta} \end{bmatrix} + x_1\begin{bmatrix} \delta_{i\alpha} \\ \delta_{i\beta} \end{bmatrix} \\
&\quad + x_2\begin{bmatrix} \dfrac{\delta_{i\alpha}^2 - \delta_{i\beta}^2}{\sqrt{6}} + \dfrac{2\delta_{i\alpha}\delta_{i\gamma}}{\sqrt{3}} \\ -\sqrt{\frac{2}{3}}\delta_{i\alpha}\delta_{i\beta} + \frac{2}{\sqrt{3}}\delta_{i\beta}\delta_{i\gamma} \end{bmatrix}
\end{aligned}
\tag{29.37}
$$

$$
\begin{aligned}
2C\frac{dx_1}{dt} &= \begin{bmatrix}\delta_{r\alpha} & \delta_{r\beta}\end{bmatrix}\begin{bmatrix} i_{r\alpha} \\ i_{r\beta} \end{bmatrix} - \begin{bmatrix}\delta_{i\alpha} & \delta_{i\beta}\end{bmatrix}\begin{bmatrix} i_{i\alpha} \\ i_{i\beta} \end{bmatrix} \\
2C\frac{dx_2}{dt} &= \frac{2}{\sqrt{3}}\begin{bmatrix}\delta_{r\alpha} & \delta_{r\beta}\end{bmatrix}\begin{bmatrix} i_{r\alpha} \\ i_{r\beta} \end{bmatrix}\delta_{r\gamma} \\
&\quad + \left[\frac{\delta_{r\alpha}^2 - \delta_{r\beta}^2}{\sqrt{6}}, -\sqrt{\frac{2}{3}}\delta_{r\alpha}\delta_{r\beta}\right]\begin{bmatrix} i_{r\alpha} \\ i_{r\beta} \end{bmatrix}\cdots \\
&\quad - \frac{2}{\sqrt{3}}\begin{bmatrix}\delta_{i\alpha} & \delta_{i\beta}\end{bmatrix}\begin{bmatrix} i_{i\alpha} \\ i_{i\beta} \end{bmatrix}\delta_{i\gamma} \\
&\quad - \left[\frac{\delta_{i\alpha}^2 - \delta_{i\beta}^2}{\sqrt{6}}, -\sqrt{\frac{2}{3}}\delta_{i\alpha}\delta_{i\beta}\right]\begin{bmatrix} i_{i\alpha} \\ i_{i\beta} \end{bmatrix}
\end{aligned}
\tag{29.38}
$$

In these final equations, it is important to point out the relation between the γ control signal and the input and output power of the DCC full converter.

29.3.5 Control

As it can be observed in Eqs. (29.36) and (29.37) the rectifier and inverter currents $i_{\alpha\beta}^r$, $i_{\alpha\beta}^i$ can be controlled separately due to the decoupling of these equations. Also it can be seen in Eq. (29.38) that the control objective on x_1 can be achieved using the normalized voltage references $\delta_{\alpha\beta}^r$ or $\delta_{\alpha\beta}^i$, and x_2 can be controlled using δ_γ^r or δ_γ^i. The implemented control consists basically of independently controlling the inverter and the rectifier. The inverter controls the voltage balance in the DC-link, whereas the rectifier controls the active and reactive power extracted from the generator.

29.3.5.1 Rectifier Control

Figure 29.37 shows the control scheme proposed for the rectifier. The objective of this controller is to make the currents of the generator such that the active and reactive power achieve the reference ones.

It is necessary to notice that the rectifier γ component of the normalized voltage is imposed to be equal to zero $\delta^r_\gamma = 0$ for not affecting on voltage balance, because this balancing is implemented on the inverter control.

29.3.5.2 Inverter Control

Inverter control is divided in two parts. The first part controls the sum of the capacitor voltages x_1, while the second part makes the difference between the capacitor voltages x_2 as small as possible.

29.3.5.3 Sum of the Capacitor Voltages Control

The controller scheme, which can be seen in Fig. 29.38, has been described before in [35], and it is appropriated for this application due to the similarities found in the equations.

The main objective of the controller is to achieve a desired value of the total DC-link voltage. Additionally, the controller can take a reactive power reference to control the power factor of the energy delivered to the utility grid.

29.3.5.4 Difference of the Capacitor Voltages Control

Avoiding the quadratic terms in δ from the equation of the difference of the capacitor voltages in Eq. (29.38), expression (29.39) is obtained:

$$\frac{dx_2}{dt} = K \cdot P^i_{ref} \cdot \delta^i_\gamma \tag{29.39}$$

where K is a constant. With this equation, the following control scheme (Fig. 29.39) is proposed:

The objective of the controller is to add a voltage reference in γ direction that depends on the sign of the power and the imbalance of the capacitors voltages.

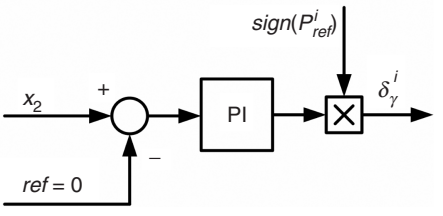

FIGURE 29.39 Proposed capacitors voltages balancing control.

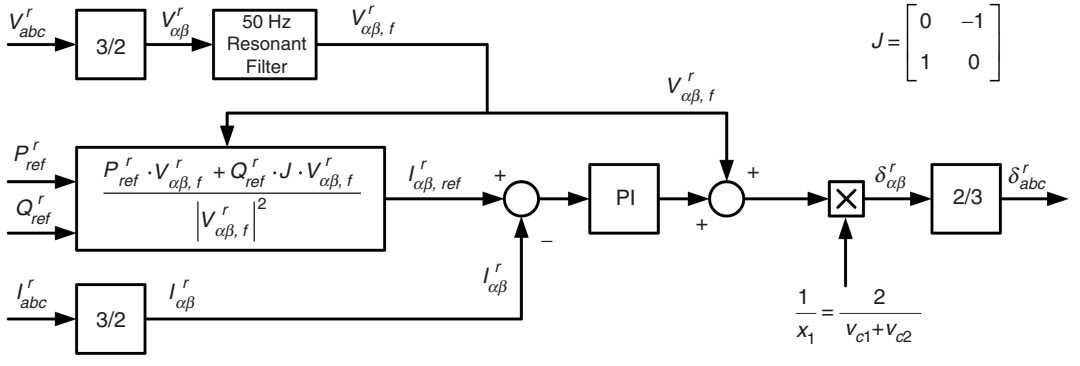

FIGURE 29.37 Control diagram of the rectifier.

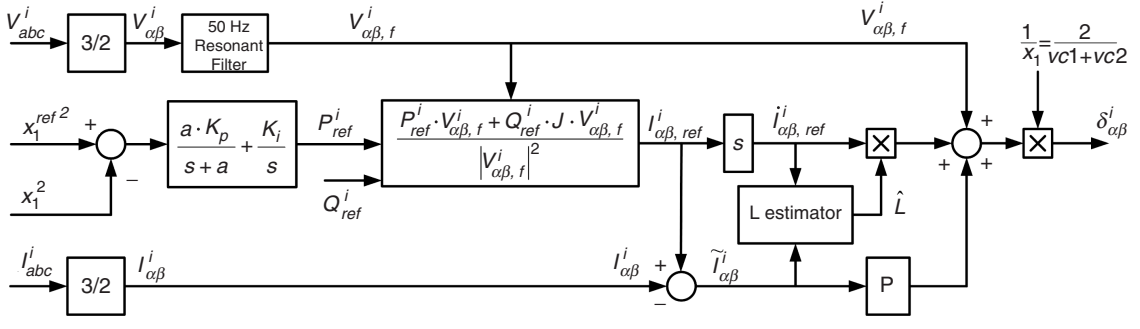

FIGURE 29.38 Inverter control scheme for the sum of the capacitors voltages.

29.3.5.5 Modulation

Finally, the normalized voltage references $\delta^r_{\alpha\beta\gamma}$ and $\delta^i_{\alpha\beta\gamma}$, obtained from the whole controllers, are translated to *abc*-coordinates and the 3D-space vector modulation algorithm [36] is used to generate the duty cycles and the switching times of power semiconductors.

29.3.6 Application Example

As it was explained before, the standards on energy quality related to renewable energy are focusing to request the plants to contribute to the general stability of the electrical system. To show that the exposed modeling strategy and control scheme can be used to meet the design specification, the electrical system of a wind turbine has been modeled. It consists of an asynchronous induction motor connected to the utility grid through a full DCC converter. The parameters of the example are: nominal power: 3 MW, switching frequency: 2.5 kHz, DC-link nominal voltage: 5 kV, and utility grid line voltage: 2.6 kV. The experiment consists of studying the behavior of the system when there is a voltage dip in the utility grid due to a short-circuit. Figure 29.40 shows the envelope of the voltage dip that has been used to carry out the results.

Figure 29.41 shows the results obtained under the voltage dip condition. Good behavior of the currents on both the sides of the full DCC converter, DC-link voltage, and energy extracted from the generator illustrates the suitability of the control scheme and the model to study the system.

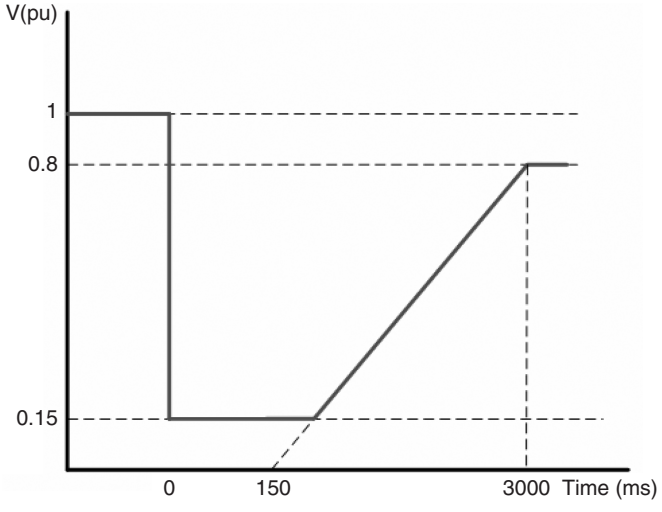

FIGURE 29.40 Voltage dip envelope.

29.4 Electrical System of a Wind Farm

29.4.1 Electrical Schematic of a Wind Farm

A wind farm is integrated by wind turbines and the substation that connect the farm to the utility grid to evacuate the electrical energy. The wind farm is arranged by string of wind turbines. Figure 29.42 shows a string compounded by several aerogenerators. These wind turbines are connected by manual switch breakers which isolate a wind turbine or it isolates the whole string. In variable-speed applications, an AC/AC power converter is used. This power converter is connected by a manual switch to the machine. The power converter includes a remote controlled switch breaker which isolates from the power transformer. The switch breaker is used for automatic reconnection after a fault. Figure 29.42 shows the transformer connection.

A schematic diagram of a typical substation is shown in Fig. 29.43. A large transformer, depicted in the figure, or several transformer connected in parallel, changes from the medium voltage to a higher voltage level. A typical voltage levels in Europe could be 20 kV/320 kV. The substation also incorporates bus bar, protections systems, measurement instrumentation, and auxiliary services circuit. Bus bar voltage measurement is made by voltage transformer. Each branch current, including several wind turbines, is measured by current transformer.

Some farms with lower rated power or connected to an isolated grid, e.g. wind-diesel systems, do not use this large transformer. The schematic of an isolated wind-diesel installation is represented in Fig. 29.44. Every power generator and load are connected to a medium voltage bus bar, in the typical range of 10–20 kV. The transformers are protected by circuit breakers that connect the lines directly to ground when open. A measurement system is used for power consumption and electrical quality control. Also auxiliaries' power supply feeds the substation equipment.

29.4.2 Protection System

Protection of wind power systems requires an understanding of system faults and their detection, as well as their safe disconnection. The protection system of a wind farm is mainly included in the substation. Circuit breaker and switchgear [37] are extensively used for overcurrent protection. New type of relay has been designed for the protection of wind farms that incorporate fixed-speed induction generators as described in [38]. A protection relay can be installed in the medium-voltage collecting line at the common point connection to the utility grid. This relay provides short-circuit protection for the collecting line and the medium-voltage (MV) and low-voltage (LV) circuits. Consequently, the relay allows wind farms to be constructed and adequately protected without the need to include fuses on the MV side of each generator–transformer.

The variable speed generator also includes digital relay protection and can be programmed for complex coordination and selectivity. This modern protection system can be used for voltage gap or sag function protection. Moreover, they can implement modern stabilization programs [39].

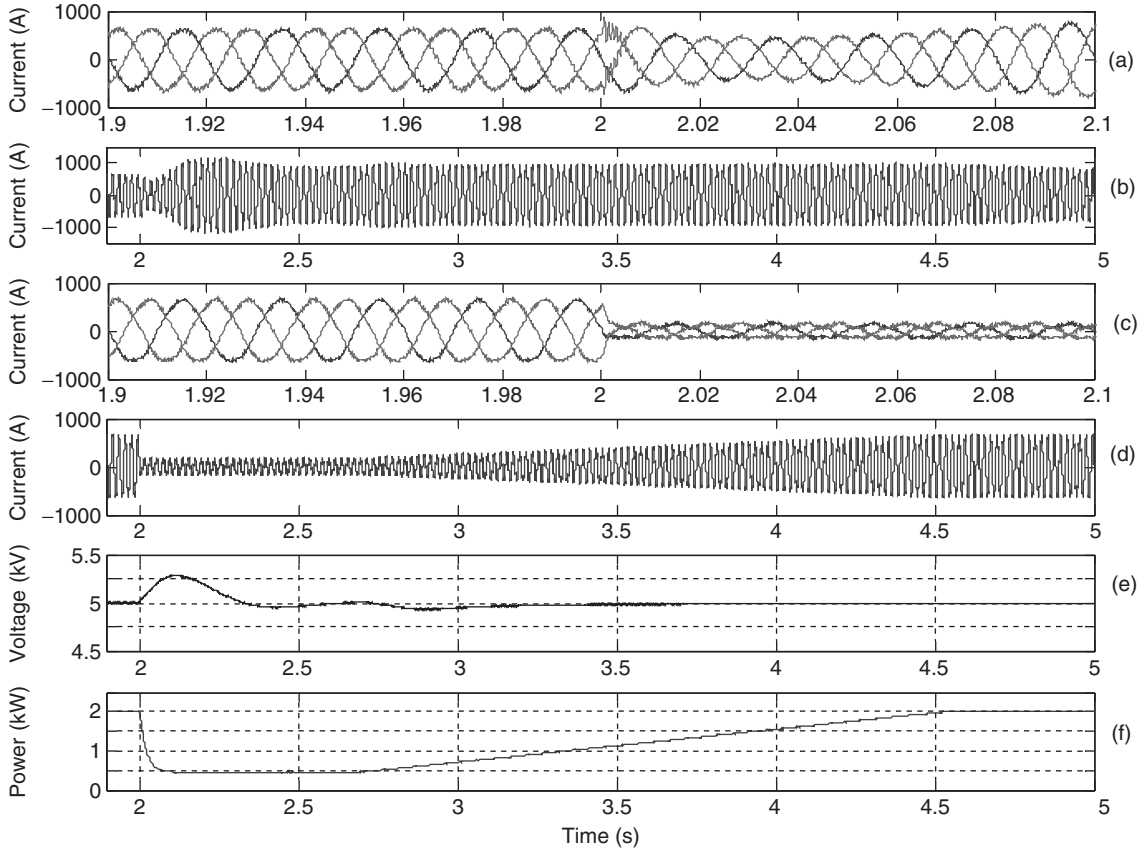

FIGURE 29.41 Response of the system to a voltage dip: (a) inverter side currents (detail); (b) inverter one phase current; (c) rectifier side currents (detail); (d) rectifier one phase current; (e) DC-link voltage; and (f) active power extracted from the generator.

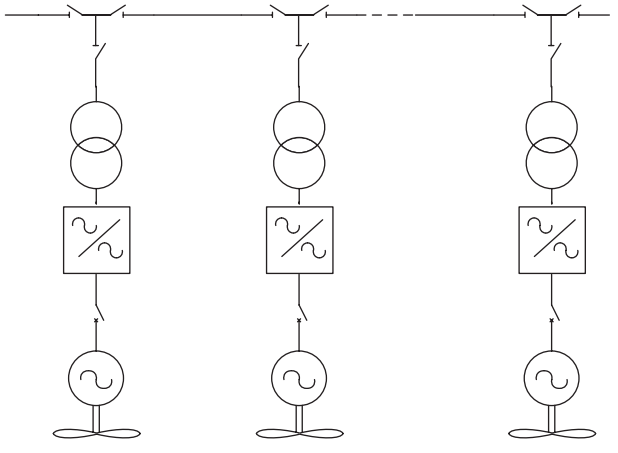

FIGURE 29.42 Typical branch composed by several wind turbines.

29.4.3 Electrical System Safety: Hazards and Safeguards

It is important to understand the hazards of electricity at the power system supply level. The safety of wind farm includes a good knowledge of electrical blast, electrocution, short circuits, overloads, ground faults, fires, lifting and pinching injuries. It is also recommended to review the principles, governmental regulations, work practices, and specialized equipment relating to electrical safety. Installers and maintenance personnel have to know the different types of "Personal Protective Equipment" through demonstrations of locking and tagging devices, protective clothing, and specialized equipment. The isolation and "Lockout Practices Procedures" for the lockout and isolation of electrical equipment can also be implemented into the existing site regulations and policies. A common practise is to use isolation transformer and grounding circuit breaker as they are being operated.

29.5 Future Trends

Future trends relating to power electronics used in wind turbine applications can be summarized in the following points:

29.5.1 Semiconductors

Improvements in the performance of power electronics variable frequency drives for wind turbine applications have been directly related to the availability of power semiconductor

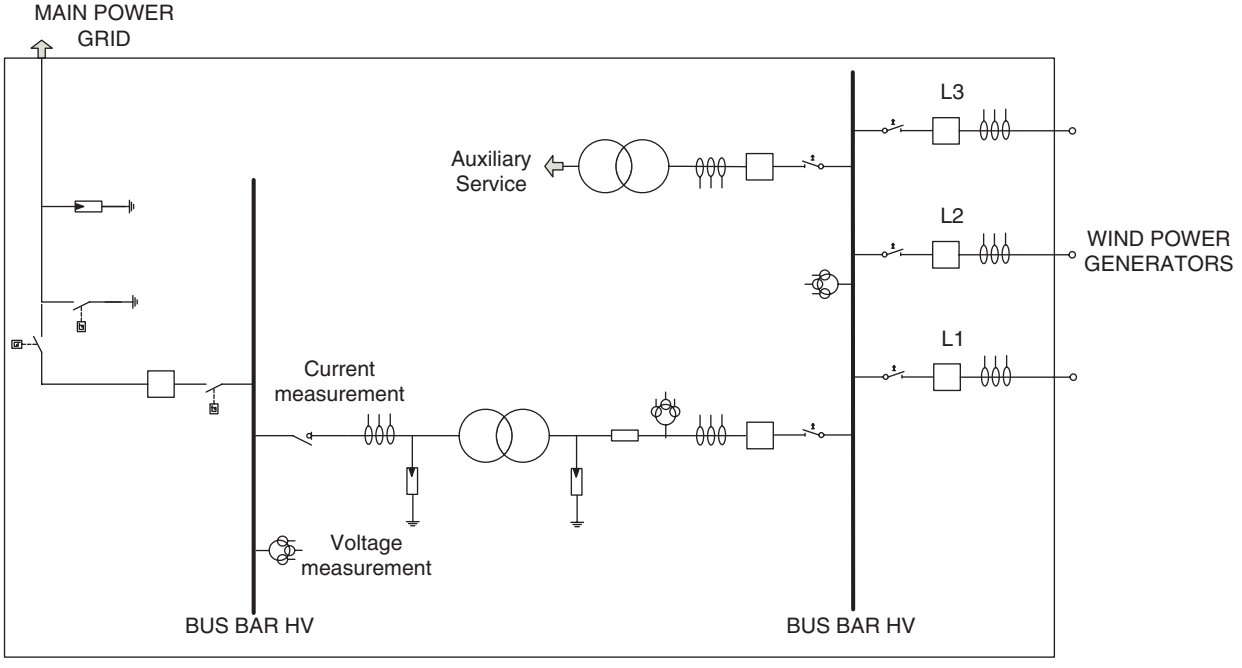

FIGURE 29.43 Schematic diagram of a typical wind farm substation.

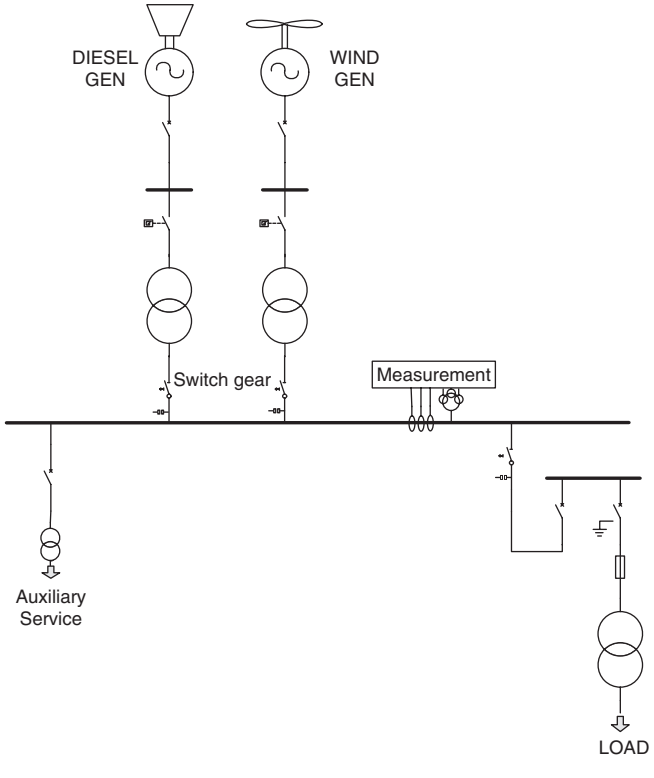

FIGURE 29.44 Schematic diagram of a wind–diesel generation system.

devices with better electrical characteristics and lower prices because the device performance determines the size, weight, and cost of the entire power electronics used as interfaces in wind turbines [8, 18, 9].

The thyristor is the component that started power electronics. It is an old device with decreasing use in medium power applications, which was replaced by turn-off components like insulated gate bipolar transistor (IGBTs). The IGBT, which can be considered as an MOS bipolar Darlington, is now the main component for power electronics, and also for wind turbine applications. They are now mature technology turn-on components adapted to very high power (6 kV–1.2 kA), and they are in competition with gate turn-off thyristor (GTO) for high power applications [40].

Recently, the integrated gated control thyristor (IGCT) has been developed, consisting of the mechanical integration of a GTO plus a delicate hard drive circuit that transforms the GTO into a modern high performance component with a large safe operation area (SOA), lower switching losses, and a short storage time [41–43].

The comparison between IGCT and IGBT for frequency converters, used especially in wind turbines is explained below:

- IGBTs have higher switching frequency than IGCTs so they introduced less distortion in the grid. Accordingly if we use two three-phase systems in parallel, it is possible to double the resulting switching frequency without increasing the power loss, hence it is possible to have a total harmonic distortion (THD) of less than 2% without special harmonic filters.

- IGCTs are made like disk devices. They have to be cooled with a cooling plate by electrical contact on the high voltage side. This is a problem because high electromagnetic emission will occur. Another point of view is the number of allowed load cycles. Heating and cooling the device will always bring mechanical stress to the silicon chip and can be destroyed. This is a serious problem, especially in wind turbine applications. On the other hand, IGBTs are built like module devices. The silicon is isolated to the cooling plate and can be connected to ground for low electromagnetic emission even with higher switching frequency. The base plate of this module is made of a special material which has exactly the same thermal behavior as silicon, so nearly no thermal stress occurs. This increases the lifetime of the device by 10-fold approximately.
- The main advantage of IGCTs versus IGBTs is that they have a lower on state voltage drop, which is about 3.0 V for a 4500 V device. In this case, the power dissipation due to a voltage drop for a 1500 kW converter will be 2400 W per phase. On the other hand, in the case of IGBT, the voltage drop is higher than IGCTs. For a 1700 V device having a drop of 5 V, and in this case the power dissipation due to the voltage drop for a 1500 kW condition will be 5 kW per phase.

In conclusion, with the present semiconductor technology, IGBTs present better characteristics, for frequency converters in general and especially for wind turbine applications.

29.5.2 Power Converters

The technology of power electronic interfaces for variable-speed wind turbines is focused on the following points:

- Development of high efficiency/high quality voltage source AC/DC/AC converter for a main connection of variable wind turbines, operating with either a permanent magnet, a synchronous or an asynchronous generator.
- Operation at a power factor around one with higher-harmonic voltage distortion less than international standards.
- The power quality of the electrical output of the wind farms may be improved by the use of advanced static var compensators STATCOM or active power filters using power semiconductors like IGBTs, IGCTs, or GTOs. These kind of power conditioning systems are a new emerging family of FACTS (flexible AC transmission system) converters, which allow improved utilization of the power network. These systems will allow wind farms to reduce voltage drops and electrical losses in the network without the possibility of transient over voltage at islanding due to self-excitation of wind generators. Moreover, power conditioning systems equipment with different control algorithm can be used to control the network voltage, which will fluctuate in response to the wind farm output if the distribution network is weak [44, 45].
- For large power wind turbine applications where it is necessary to increase the voltage level of the semiconductor of the power electronic interface, multilevel power converter technology is emerging as a new breed of power converter options for high-power applications. The general structure of the multilevel converter is to synthesize a sinusoidal voltage from several levels of voltages, typically obtained from capacitor voltage sources. Additionally, these converters have better performance and controllability because they use more than two voltage levels [46–48].

29.5.3 Control Algorithms

A variable pitch and speed wind turbine is a very complex non-lineal system. The control problem is more difficult to solve because some performance objectives, such as maximum power captured, minimum mechanical stress, constant speed, and power constant counteract each other. To solve this problem, a Fuzzy Logic control has recently been proposed. The Fuzzy Logic controller implements a rule-based structure [49] that can be easily adapted in order to optimize performance control objectives and has been widely used in introduction motor control applications [50–53]. In [54], a Fuzzy Logic controller is used to optimize the power captured using maximum power tracking algorithms. Other original structures have been proposed in [55]. The structure implements different control strategies depending on the rotor speed and generates a current torque control action. Presently, more complex control structures are being researched.

29.5.4 Offshore and Onshore Wind Turbines

One of the main trends in wind turbine technology is offshore installations. There are great wind resources at sea for installing wind turbines in many areas where the depth of the sea is relatively shallow. There are several demonstration plants that have had extremely positive results, so interest has increased in installing offshore wind farms, because of the development of large commercial power MW wind turbines. Offshore wind turbines may have slightly more favorable energy balance than onshore turbines, depending on local wind conditions. In places where onshore wind turbines are typically placed on flat terrain, offshore wind turbines will generally yield some 50% more energy than a turbine placed on a nearby onshore site. The reason is the low roughness of the sea surface. On the other hand, the construction and installation of a foundation requires 50% more energy than onshore turbines. It should be remembered, however, that offshore wind turbines have a longer life expectancy, around 25 to 30 years, than onshore turbines. The reason is that the low turbulence at sea gives lower fatigue loads on the wind turbine.

From a power electronics point of view, offshore wind turbines are interesting because, under certain circumstances, they become desirable to transmit the generated power to the load center over DC transmission lines (HVDC). This alternative becomes economically attractive versus AC transmission when a large amount of power is to be transmitted over a long distance from a remote wind farm to the load center [8]. Moreover, the transient stability and the dynamic damping of the electrical system oscillations can be improved by HVDC transmissions.

Nomenclature

C_{dc}	DC link capacitor.
$C_p(\lambda, \beta)$	Power coefficient at tip speed ratio λ and pitch β.
e_{rg}, e_{sg}, e_{tg}	Instantaneous values of grid voltages.
e_α, e_β	Grid voltages expressed in an orthogonal reference frame.
f_1	Excitation frequency (the same as the grid frequency) in hertz.
f_2	Frequency of the voltage supplied to the rotor of machine 2 in hertz.
G	Gearbox ratio.
i_{dc}	DC inductor current of the step-up converter.
i_{dc}^{ref}	Desired DC inductor current of the step-up converter.
i_{dse}, i_{qse}	Instantaneous values of the direct and quadrature-axis stator current components, respectively, and expressed in rotor-flux-oriented reference frame.
$i_{dse}^{ref}, i_{qse}^{ref}$	Desired instantaneous values of the direct and quadrature-axis stator current components, respectively, and expressed in rotor-flux-oriented reference frame.
i_{dsr}, i_{qsr}	Stator current components established in the rotor reference frame.
$i_{dsr}^{ref}, i_{qsr}^{ref}$	Desired stator current components established in the rotor reference frame.
i_{ds}, i_{qs}	Instantaneous values of the direct and quadrature-axis stator current components, respectively, and expressed in the rotor reference phase.
i_{Ds}, i_{Qs}	Instantaneous values of the direct and quadrature-axis stator current components, respectively, and expressed in the stator reference frame.
$i_{Ds}^{ref}, i_{Qs}^{ref}$	Desired direct and quadrature-axis stator current components expressed in the stator reference frame.
i_{exc}	Synchronous generator excitation current.
i_{exc}^{ref}	Desired synchronous generator excitation current.
$i_{R_g}^{ref}, i_{S_g}^{ref}, i_{T_g}^{ref}$	Desired stator current.
$i_{R_r}, i_{S_r}, i_{T_r}$	Rotor current.
$i_{R_s}, i_{S_s}, i_{T_s}$	Stator current.
$i_{R_s}^{ref}, i_{S_s}^{ref}, i_{T_s}^{ref}$	Desired stator current.
i_{rg}, i_{sg}, i_{tg}	Public grid phase currents.
i_m^{ref}	Desired magnetizing current.
i_m	Magnetizing current.
i_{dsm}, i_{qsm}	Instantaneous values of the direct and quadrature-axis magnetizing stator current components, respectively, and expressed in the magnetizing current-oriented reference frame.
J	Total inertia of the system referred to the high speed shaft.
k_{ws}, k_{wr}	Winding factors of rotor and stator.
L_m	Coupled inductance.
L_{AC}	Inductance of inductors at the AC side of the inverter.
L_S, L_r	Stator and rotor windings inductances.
L_{DC}	Inductance of the step-up chopper.
n	Turns ratio of the machine. $n = k_{ws} \cdot n_s / k_{wr} \cdot n_r$
n_s, n_r	Number of turns of each rotor and stator phase.
N_1	Angular speed of the magnetic field (synchronous speed) expressed in rpm.
N_r	Angular speed of the generator rotor expressed in rpm.
p	Number of pole pairs.
p_1, p_2	Number of pole pairs of machine number 1 and 2.
P_1	Electrical power in the stator of principal machine number 1.
P_2	Electrical power in the stator of auxiliary machine number 2.
P_e	Electrical generated power.
P_m	Mechanical power in the low speed shaft.
P_{max}	Generated maximum power.
P_{rate}	Generator rate power.
P_S, Q_S	Active and reactive power through the stator.
P_S^{ref}, Q_S^{ref}	Desired active and reactive power through the stator.
P_{slip}	Slip power.
P_w	Available wind power.
p^{ref}, q^{ref}	Desired real power and desired reactive power on the grid side.
Q_e	Electromagnetic torque of the machine.
Q_e^{ref}	Desired electromagnetic torque of the machine.
Q_L	Torque in the low speed shaft.
Q_{rate}	Generator rate torque.
Q_t	Torque in the high speed shaft.
R	Rotor radius.
R_S, R_r	Stator and rotor winding resistors.
s	Slip.
$s_1 = \omega_1 - \omega_r / \omega_1$	Slips of machine principal number 1.
$s_2 = \omega_2 - \omega_r / \omega_2$	Slips of machine principal number 2.
T_s, T_r	Stator and rotor time constants, respectively.
$u_{dse}^{ref}, u_{qse}^{ref}$	Desired direct and quadrature-axis stator voltage expressed in the rotor-flux-oriented reference frame.
$u_{Ds}^{ref}, u_{Qs}^{ref}$	Desired direct and quadrature-axis stator voltage expressed in the stator reference frame.

$u_{R_r}, u_{S_r}, u_{T_r}$ Rotor voltage.
$u_{R_s}, u_{S_s}, u_{T_s}$ Stator voltage.
$u_{R_s}^{ref}, u_{S_s}^{ref}, u_{T_s}^{ref}$ Desired stator voltage.
u_r, i_r, λ_r Rotor voltage, current, and flux, respectively, referred to a reference frame that rotates with the rotor.
u'_r, i'_r, λ'_r Rotor voltage, current, and flux, respectively, referred to a reference frame fixed with the stator.
u_s, i_s, λ_s Stator voltage, current, and flux, respectively, referred to a reference frame fixed with the stator.
u_{ds}, u_{qs} Direct and quadrature-axis stator voltage expressed in the magnetizing current reference frame.
v_{rat} Rated wind speed.
$v_{p_{max}}$ Maximum power wind speed.
v_{start} Start wind speed.
v_{stop} Stop wind speed.
v_w Wind speed.
V_{dc} DC-Link capacitor voltage.
V_{dc}^{ref} Desired DC-Link capacitor voltage.
V_{st}^{max} Maximum RMS stator voltage of the synchronous generator.
V_{st}^{min} Maximum RMS stator voltage of the synchronous generator.
β Pitch angle.
β^{ref} Desired pitch angle.
δ Load angle.
$\lambda = \omega \cdot R/V_v$ Tip speed ratio.
λ_{opt} Optimal tip speed ratio.
λ_m Magnetizing flux linkage vector.
$\lambda_{md}, \lambda_{mq}$ Instantaneous values of the direct and quadrature axis magnetizing flux linkage components expressed in the rotor reference frame.
$|\lambda_m|$ Estimated modulus of magnetizing flux linkage vector.
$\left|\lambda_m^{ref}\right|$ Desired modulus of magnetizing flux linkage vector.
η Electrical performance.
η_r Phase angle of the rotor flux linkage space phasor with respect to the direct axis of the stator reference frame.
θ_e Magnetizing current angle.
θ_{sl} Angle corresponding to the angular slip frequency.
θ_r Rotor angle.
ρ Air density.
$\omega_1 = 2\pi f_1/p_1$ Angular speed of the rotating magnetic flux produced in the stator of machine 1 relative to the stator.
$\omega_2 = 2\pi f_2/p_2$ Angular speed of the rotating magnetic flux produced in the rotor of machine 2 relative to the rotor.
ω_L Low-speed shaft angular speed.
ω_r Angular speed of the generator rotor.
ω_r^{ref} Reference rotor speed.
ω_r^{max} Maximum angular speed of the synchronous generator.
ω_r^{min} Minimum angular speed of the synchronous generator.
ω_Q^{ref} Desired angular speed for the torque controller.
ω_β^{ref} Desired angular speed for the pitch controller.
ω_r^{rate} Rated value of the rotor speed.
ω_e Electrical angular speed of the magnetizing current reference frame.

References

1. S. Heier, "Grid Integration of Wind Energy Conversion Systems". Chichester, Sussex (UK): John Wiley & Sons, 1998.
2. G.L. Johnson, "Wind Energy Systems". Englewood Cliffs, NJ (US): Prentice-Hall, INC., 1985.
3. P. Vas, "Vector Control of AC Machines", NY (US): Oxford Clarendon Press, 1990.
4. V. Subrahmanyam, "Electric Drives. Concepts and Applications". NY (US): MacGraw-Hill, 1996.
5. M. Alatalo, M. Sc, and T. Svensson, "Variable Speed Direct-Driven PM-Generator With a PWM Controlled Current Source Inverter". *European Community Wind Energy Conference.* March 1993. Lùbeck-Travemùnde, Germany.
6. P. Vas, "Sensorless Vector and Direct Torque Control". NY (US): Oxford University Press, 1998.
7. Chee-Mun Ong. "Dynamic Simulation of Electric Machinery Using Matlab/Simulink". Prentice Hall PTR, 1998.
8. N. Mohan, T.M. Undeland, and W.P. Robbins, "Power Electronics, Converters, Applications, and Design". Second edition, John Wiley & Sons, INC., 1995.
9. R.E. Tarter. "Solid-State Power Conversion Handbook". John Wiley & Sons, Inc., 1993.
10. B.K. Bose, "Power Electronics and Variable Frequency Drives. Technology and Applications". IEEE Press, 1997.
11. S.A. Papathanassiou and M.P. Papadopoulos, "A Comparison of Variable Speed Wind Turbine Configurations". *Wind Energy Conference.* March 1999, France.
12. D.S. Zinger and E. Muljadi. "Annualized Wind Energy Improvement Using Variable Speeds". *IEEE Transactions on Industry Applications*, Vol. 33, No. 6, Nov–Dec 1997.
13. K. Pierce, "Control Method for Improved Energy Capture below Rated Power". *Third edition ASME/JSME Joint Fluids Engineering Conference.* July, 1999. San Francisco, California.
14. *Theory Manual.* E.A Bossanyi, "Bladed for Windows". Garrad Hassan and Partners Limited. September 1997.
15. E. Muljadi, K. Pierce, and P. Migliore, "Control Strategy for Variable-Speed, Stall-Regulated Wind Turbines". *American Controls Conference.* June 1998. Philadelphia, NREL.
16. A.D. Simmons, L.L. Freris, and J.A.M. Bleijs, "Comparison of Energy Capture and Structural Implementaions of Various Policies of Controlling Wind Turbines". *Wind Energy: Technology and Implementation.* 1991. (Amsterdam EWEC'91).
17. W.E. Leithead, S. de la Salle, and D. Reardon, "Wind Turbine Control Objectives and Design". *European Community Wind Energy Conference.* September 1990. Madrid, Spain.

18. M.H. Rashid, *Power Electronics. Circuits, Devices, and Applications*. Second edition. Englewood Cliffs, NJ(US): Prentice Hall, 1993.
19. H. Akagi, A. Nabae, and S. Atoh, "Control Strategy of Active Power Filters Using Multiple Voltage-Source PWM Converters". *IEEE Trans. Ind. Applications*, Vol. IA-22, No. 3, pp. 460–465, May–June 1986.
20. S. Bhowmik, R. Spée, and J.H.R. Enslin, "Performance Optimization for Doubly Fed Wind Power Generation Systems". *IEEE Transactions on Industry Applications,* Vol. 35, No. 4, July–August 1999.
21. B. Hopfensperger, D.J. Atkinson, and R.A. Lakin, "Application of Vector Control to the Cascaded Induction Machine for Wind Power Generation Schemes". *7th IEE European on Power Electronics, EPE'97*. September 1997. Trondheim (Norway).
22. P.O. 12.3 "Propuesta sobre requisitos de respuesta frente a huecos de tensión de las instalaciones eólica". Red Eléctrica de España, S.A. October 2005.
23. C. Rasmussen, P. Jorgensen, and J. Havsager, "Integration of Wind Power in the Grid in Eastern Denmark". In *Proc 4th International Workshop on Large-scale Integration of Wind Power and Transmission Network for Offshore Wind Farm*, 20–21 October 2003, Billund, Denmark.
24. E.ON Netz Grid Code, Bayreuth; E.ON Netz GmbH. Germany, 1 August 2003.
25. M. Johan and de Hann Sjoerd W.H. "Ridethrough of Wind Turbines with Doubly-fed Induction Generator During a Voltage Dip". *IEEE Transaction on Energy Conversion*, Vol. 20, No. 2. June 2005.
26. X. Bing, F. Brendan, and F. Damian, "Study of Fault Ride Through for DFIG Wind Turbines". *IEEE Transaction on Energy Conversion*, Vol. 20, No. 2. June 2005.
27. International Electrotechnical Commission. Draft IEC 61400-21: Power Quality Requirements for Grid Connected Wind Turbines. Committee Draft (CD). December 1998.
28. D. Foussekis, F. Kokkalidis, S. Tentzevakis, and D. Agoris, "Power Quality Measurement on Different Type of Wind Turbines Operating in the Same Wind Farm". EWEC 2003.
29. S. Poul, G. Gert, S. Fritz, R. Niel, D. Willie, K. Maria, M. Evangelis, and L. Ake, "Standards for Measurements and Testing of Wind Turbine Power Quality". EWEC 1999.
30. International Electrotechnical Commission, IEC Standard, Amendment 1 to Publication 61000-4-7, Electromagnetic Compatibility, General Guide on Harmonics and Inter-harmonics Measurements and Instrumentation, 1997.
31. International Electrotechnical Commission, IEC Standard, Publication 61000-3-6, Electromagnetic Compatibility, Assessment of Emission Limits for Distorting Loads in MV and HV Power Systems, 1996.
32. L. Ake, S. Poul, and S. Fritz, *Grid Impact of Variable Speed Wind Turbines*. EWEC' 1999.
33. A. Nabae, H. Akagi, and I. Takahashi, "A New Neutral-Point-Clamped PWM Inverter". *IEEE Transactions on Industry Applications*, Vol. IA-17, No. 5, pp. 518–523, September/October 1981.
34. G. Escobar, J. Leyva, J.M. Carrasco, E. Galvan, R. Portillo, M.M. Prats, and L.G. Franquelo, "Modeling of a Three Level Converter Used in a Synchronous Rectifier Application", in *Proc. Power Electronics Specialists Conference, PESC'04*, Aachen, Germany, Vol. 6, pp. 4306–4311, 2004.
35. G. Escobar, J. Leyva-Ramos, J. M. Carrasco, E. Galvan, R. Portillo, M.M. Prats, and L.G. Franquelo, "Control of a Three Level Converter Used as a Synchronous Rectifier". *2004 IEEE 35th Annual Power Electronics Specialists Conference, PESC'04*, Vol. 5, pp. 3458–3464, June 20–25, 2004.
36. M.M. Prats, L.G. Franquelo, R. Portillo, J.I. León, E. Galván, and J.M. Carrasco, "A Three Dimensional Space Vector Modulation Generalized Algorithm for Multilevel Converters". *IEEE Power Electronics Letters*, Vol. 1, pp. 110–114, 2003.
37. W.D. Goodwin, "High-voltage Auxiliary Switchgear for Power Stations". *Power Engineering Journal* [see also Power Engineer], Vol. 3, No. 3, pp. 145–154, May 1989.
38. S.J. Haslam, P.A. Crossley, and N. Jenkins, "Design and Evaluation of a Wind Farm Protection Relay". Generation, Transmission and Distribution, *IEE Proceedings*, Vol. 146, No. 1, pp. 37–44, January 1999, Digital Object Identifier 10.1049/ip-gtd:19990045.
39. M.P. Palsson, T. Toftevaag, K. Uhlen, and J.O.G. Tande, "Large-scale Wind Power Integration and Voltage Stability Limits in Regional Networks". Power Engineering Society Summer Meeting, *IEEE Proceedings*, Vol. 2, pp. 762–769, 2002. Digital Object Identifier 10.1109/PESS.2002.1043417.
40. J.M. Peter, "Main Future Trends for Power Semiconductors from the State of the Art to Future Trends". *Power Conversion Intelligent Motion (PCIM'99)*. Nürnberg, June 1999.
41. H. Grüning, B. Ødegård, J. Rees, A. Weber, E. Carroll, and S. Eicher, "High Power Hard-Driven GTO Module for 4.5kV/3kA Snubberless Operations". *PCI Europe Proceedings,* Nürnberg, 1996.
42. A. Jaecklin, "Integration of Power Components – State of the Art and Trends". *European Power Electronic Conference EPE'97*. Trondheim, 1997.
43. H.R. Zeller, "High Power Components from the State of the Art to Future Trends". *PCIM Europe Proceedings*, Nürnberg, 1998.
44. J.M. Carrasco, M. Perales, B. Ruiz, E. Galván, L.G. Franquelo, S. Gutiérrez, and E. Gonzalez "DSP Control of an Active Power Line Conditioning System". *7th IEE European Conference on Power Electronics, EPE'97*. Trondheim (Norway). September 1997.
45. J. Balcells, M. Lamich, and D. González, "Parallel Active Filter Based on a Three Level Inverter". *European Power Electronic Conference EPE'99*. Laussane, 1999.
46. R. Teodorescu, F. Blaabjerg, J.K. Pedersen, E. Cengelci, S.U. Sulistijo, B.O. Woo, and P. Enjeti, "Multilevel Converters – A Survey", *European Power Electronic Conference EPE'99*. Lausanne, September 1999.
47. K. Oguchi, T. Karaki, and N. Hoshi, "Space Vector of Output Voltages of Reactor-Coupled Three Phase Multilevel Voltage-Source Inverters". *European Power Electronic Conference EPE´99*. Lausanne, September 1999.
48. J.-S. Lai and F.Z. Peng, "Multilevel Converters – A New Breed of Power Converters". *IEEE Transactions on Industry Application*, Vol. 32, No. 3. May–June 1996.
49. M. Sugeno, "An Introductory Survey of Fuzzy Control". *Information Sciences*, 36, pp. 59–83, 1985.
50. E. Galván, A. Torralba, F. Barrero, M.A. Aguirre, and L.G. Franquelo, "Fuzzy-Logic Based Control of an Induction Motor". *Industrial Fuzzy Control and Applications*. Tarrasa (Spain), March 1993.
51. E. Galván, A. Torralba, F. Barrero, M.A. Aguirre, and L.G. Franquelo, "A Robust Speed Control of AC Motor Drives based on Fuzzy

Reasoning". *Industry Application Society (IAS)*. Toronto (Canada), October 1993.

52. F. Barrero, E. Galván, A. Torralba, and L.G. Franquelo, "Fuzzy Selftuning System for Induction Motor Controllers". *IEE European Conference on Power Electronics, EPE'95*. Seville (Spain), September 1995.
53. F. Barrero, A. Torralba, E. Galván and L.G. Franquelo, "A Switching Fuzzy Controller for Induction Motors with Self-tunning Capability". *Int. Con. on Industrial Electronics, IECON'95*. Orlando, Florida (USA), November 1995.
54. M. Godoy Simoes, B.K. Bose, and R.J. Spiegel "Fuzzy Logic Based Intelligent Control of a Variable Speed Cage Machine Wind Generation System". *IEEE Transaction on Power Electronics*, Vol. 12, No. 1, pp 87–95, January 1997.
55. M. Perales, J. Pérez, F. Barrero, J.L. Mora, E. Galván, J.M Carrasco, L.G. Franquelo, D. de la Cruz, L. Fernández, and A. Zazo, "A New Fuzzy Based Approach for a Variable Speed, Variable Pitch Wind Turbine". *8th International Fuzzy Systems Association World Congress*. IFSA'99.